R. & M. No. 3405

MINISTRY OF AVIATION

AERONAUTICAL RESEARCH COUNCIL
REPORTS AND MEMORANDA

An Experimental High-Temperature Turbine (No. 126)

Part I.—The Cooling Performance of a Set of Extruded Air-Cooled Turbine Blades

By D. E. Fray and J. F. Barnes

Part II.—The Effects of Cooling on the Aerodynamic Performance

By J. F. Barnes and D. E. Fray

LONDON: HER MAJESTY'S STATIONERY OFFICE
1965
PRICE £1 0s. 0d. NET

An Experimental High-Temperature Turbine (No. 126)

COMMUNICATED BY THE DEPUTY CONTROLLER AIRCRAFT (RESEARCH AND DEVELOPMENT), MINISTRY OF AVIATION

*Reports and Memoranda No. 3405**
December, 1962

Part I.—The Cooling Performance of a Set of Extruded Air-Cooled Turbine Blades

By D. E. FRAY and J. F. BARNES

Summary.

Cooling characteristics are given in terms of the variation of average blade temperature at mid-span with cooling-flow rate, Reynolds number, gas/cooling-air absolute temperature ratio, and, for the rotor, gas-stream incidence. Chordwise and spanwise variations of blade temperature are also presented.

Measured pressure-drop characteristics indicate that in a gas-turbine engine, with the cooling-air inlet pressure equal to the turbine gas inlet total pressure, cooling flows roughly equal to 1·8 per cent and 3·0 per cent of the main gas flow could be passed through the nozzle and rotor blades respectively, giving average relative temperatures at mid-span of approximately 0·6 in each instance.

Comparisons with theoretical estimates of blade temperature show that the external heat-transfer rates to the nozzle blades agreed well with those measured on similar blades in cascade tests. For the rotor blades the external heat-transfer rates appear to have been between those predicted from cascade and earlier turbine test data. From the measured effects of Reynolds number on blade temperature it seems that approximately equal areas of laminar and turbulent boundary layer existed on both nozzle and rotor blades, and that as the turbine inlet temperature was raised, the extent of the turbulent layer tended to increase.

LIST OF CONTENTS

* Part I replaces N.G.T.E. Report No. R.249—A.R.C. 24 565.
Part II replaces N.G.T.E. Report No. R.250—A.R.C. 24 566.

LIST OF APPENDICES

LIST OF ILLUSTRATIONS

1. *Introduction.*

A new experimental high-temperature turbine has been described in Ref. 1. This turbine was designed and built to obtain data for a method of blade cooling. Such techniques are finding increasing application in gas turbines, particularly aircraft engines, and offer potential for yet further substantial increase in operating flame temperatures. Work on an earlier turbine has been recorded by Ainley, Waldren and Hughes[2], and gives experimental results for a type of internally air-cooled turbine blade with a multiplicity of small-diameter coolant passages. These blades were manufactured by a sintering process. With the advent of different methods for the manufacture of air-cooled blades, in particular the method of extrusion and cold rolling, and in view of certain limitations described in Ref. 2, it was necessary to obtain further test data. Extruded and cold rolled blades have relatively few cooling passages when compared with the previously sintered blade intended for the same duty. Also, instead of being nearly circular in cross-section, the cooling passages in the extruded blade are of elliptical form (with ratios of major to minor axes up to ten).

It had originally been planned that turbine testing would commence with extruded air-cooled blades in both nozzle and rotor blade rows. Owing to the time taken in developing the manufacturing process of the cooled rotor blades, it was decided to manufacture and install a set of solid rotor blades, with the same external profile as the extruded blades, in order to obtain the initial test experience reported in Ref. 1 without any delay. During the tests with the uncooled rotor blades, the turbine inlet gas temperature was limited to approximately 1100°K, but this enabled a limited investigation to be made of the cooling characteristics of the extruded nozzle blades.

Now the degree of cooling obtained in a blade whose geometry is fixed depends principally upon the temperature difference between the main gas stream and the cooling air and upon the ratio of the cooling-air flow passed through the blades to the main gas flow passing through the blade row. The cooling performance also depends on the gas-flow Reynolds number, the ratio of the absolute temperatures of the gas and cooling air, and, for the rotors, the angle of incidence of the approaching gas stream. Later tests with extruded cooled rotor and nozzle blades allowed a full investigation to be made into the cooling performance of the rotor blade, including pressure-drop characteristics, over a wide range of the above parameters. In addition the range of tests was extended to higher inlet gas temperatures (up to 1500°K).

A comparison is made between the results obtained from these turbine tests and those by theoretical methods[3], using experimental data on heat transfer [4, 5].

2. *Turbine Blading.*

Fig. 1 illustrates the assembly of the turbine blading and the cooling-air flows to the turbine stage. The rig as a whole was designed to provide a turbine stage capable of running at a maximum speed of 13 300 rev/min and at a maximum inlet gas temperature of 1600°K (assuming the blade cooling to be sufficiently good for the rotor blades to be capable of withstanding these conditions).

Both turbine builds incorporated extruded air-cooled nozzle blades of untwisted constant-section profile (Fig. 2). The blades were manufactured from extruded Nimonic 90 strip with welded root and tip platforms, and each blade contained 16 elliptical cooling passages running spanwise through the blade. Ref. 5 showed that the chordwise distribution of cooling air in the passages would probably be non-uniform if there was a clearance space at the tip of the blade, and Ref. 2 demonstrated that a serious loss of efficiency could be attributed to such a nozzle clearance space in tests on an earlier experimental cooled turbine. For these reasons a shrouded-tip design was used.

The first set of rotor blades, for the reasons given in the Introduction, were uncooled, and of untwisted constant-section profile, machined from Nimonic 80A material. The cooled rotor blades were of identical profile to the solid blades, but with 13 elliptical cooling passages and were machined from Nimonic 90 material (Fig. 3). In order to provide adequate strength in the rotor-blade root fixing to withstand the centrifugal loading, the final extrusions for the rotor blades were of such a shape that the root fixings could be machined integral with the blades. Details of the blades are given in Appendix II, and the positions in the blades in which thermocouples were fitted to measure blade metal temperatures are given in Figs. 2 and 3.

3. *Scope of Tests.*

The primary objective of the tests was the determination of the cooling characteristics of the blades over a wide range of gas-flow Reynolds numbers. To this end the majority of testing was carried out with the turbine exhausting at atmospheric pressure, but in order to cover the higher Reynolds number range ($1{\cdot}2 \times 10^5$ to $1{\cdot}6 \times 10^5$ on to the rotor blades), restrictor plates were fitted in each of the exhaust ducts to raise the pressure level in the system. Conversely, an ejector was coupled to the exhaust ducts to lower the pressure level in the turbine in order to complete the tests in the lower part of the range ($0{\cdot}65 \times 10^5$ to $0{\cdot}8 \times 10^5$). The range of mean inlet gas temperature was initially from 900°K to 1300°K coupled with a cooling-air inlet temperature of approximately 400°K for the nozzle blades and 310°K for the rotor blades. Over this range of gas temperatures, the metal temperatures reached by the blades were such that the cooling-flow ratio, defined as the ratio cooling-air flow to blades/main gas-stream flow, could be varied from approximately $0{\cdot}04$ down to $0{\cdot}005$.

The effect of incidence was covered at one Reynolds number, gas temperature level and cooling-air flow ratio.

The cooling performance of the nozzle blades was investigated by setting the turbine operating conditions to a selected gas inlet temperature and gas mass flow, and then by varying the nozzle-blade cooling quantity in a number of steps from approximately 4 per cent of the main-stream flow down to nearly zero. Readings were taken at each point of blade metal temperatures, turbine pressures and temperatures and coolant-flow quantities.

Special tests were made to examine closely the metal temperatures obtained when no cooling air was passed through the cooling passages. Earlier tests suggested that probably there was some leakage of cooling air into the nozzle-blade coolant passages from other parts of the turbine structure. The coolant passages of certain instrumented blades were therefore sealed with Sauereisen cement and tests carried out at gas temperatures up to 900°K. The test points so obtained are shown on Fig. 7 and discussed in Section 4.1.

To examine the rotor-blade cooling characteristics, the turbine was operated at the inlet gas temperature and gas flow to give the required gas-flow Reynolds number, and the brake load was adjusted to give the necessary turbine speed for zero incidence on to the rotor blades. The rotor-blade coolant flow was then progressively reduced from approximately 3 per cent of the main gas-stream flow down to nearly zero flow. At each test condition, readings were taken of blade metal temperatures, turbine pressures and temperatures and coolant-flow quantities. While operating the turbine under suction conditions (low Reynolds number), it was necessary to take special precautions to prevent leakage of air into the cooling-air passages, and a calibration of the air seals on the rotor shaft at the cooling-air entry chamber was necessary.

4. *Discussion of Results.*

4.1. *Nozzle-Blade Cooling Characteristics.*

The outlet gas temperature distribution from the combustion chamber was not uniform at part loads and, for convenience, the instrumented nozzle blades had to be divided into two groups. Therefore gas-temperature radial traverses were made just upstream of each of these groups and the corrected mean value taken as the 'effective' gas temperature on to the nozzle blades. This effective gas temperature was calculated as follows:

$$T_{(\text{effective})} = T_{c/c}\left\{1 - \frac{0{\cdot}14\dfrac{\gamma-1}{2}M_0^2}{1+\dfrac{\gamma-1}{2}M_0^2}\right\}$$

The notation is given in Appendix I.

The blade relative temperature defined as

$$\frac{\text{blade temperature} - \text{cooling-air temperature at inlet to the blade}}{\text{'effective' gas temperature} - \text{cooling-air temperature at inlet to the blade}}$$

was then calculated for each cooling-flow ratio. In order to illustrate the cooling performance of the blades it is convenient to give the results in terms of the average blade relative temperature over a chordwise section at the mean diameter. This average value was determined in the following manner. The cooling holes were assumed to divide the blade metal at any spanwise station into two distinct portions, the outer portion at an area mean of the measured surface temperatures and the central portion or 'core' at the arithmetic mean of the camber-line temperatures. The cross-section area of each portion of metal was then calculated and the resultant chordwise average relative temperature determined.

Fig. 4 illustrates the variation of this average blade relative temperature with cooling-flow ratio at several values of gas to cooling-air temperature ratio. It will be observed that the blade relative temperature at zero cooling flow does not reach a value of unity. This is caused by spanwise conduction at both blade root and tip. The theoretical estimate for the variation of relative temperature with cooling-flow ratio at gas to cooling-air temperature ratio of 2 is also shown. The gas to blade heat transfer for this estimate was based on cascade tests[5]. This curve attains a blade relative temperature of unity at zero cooling flow because no allowance was made in the calculations for the effects of spanwise conduction. However, reasonable agreement between the theoretical and measured values is demonstrated at cooling-flow ratios between 0·005 and 0·03, indicating that for gas to cooling-air temperature ratios of about 2, the external heat-transfer rates measured in this investigation were similar to those measured in the cascade tests of Ref. 5.

The variation of nozzle-blade relative temperature with gas to cooling-air temperature ratio is shown in Fig. 5, indicating that some loss in cooling effectiveness occurs as the temperature ratio increases. The plotted points are for a blade-coolant ratio of 0·02 and a gas-stream Reynolds number of 2×10^5. Relative temperatures have been calculated by the method given in Appendix III, using what are believed to be the upper and lower possible limits to external heat-transfer rates[3] for this turbine blade profile. The effect of temperature ratio as given by the experimental data is more pronounced than that predicted by the theoretical calculation. It is suggested that this may be associated with a change in boundary-layer condition at the higher temperature ratios due to greater

turbulence in the gas stream. It is reasonable to expect that an increase of combustion gas temperature should be accompanied by such a rise in turbulence level and measurements made in cascade tests[6] on a blade of identical section but longer span tend to confirm this suggestion.

Between the values of temperature ratio of 2·15 and 3·0 (the range covered by the tests), an increase in blade relative temperature of 0·07 occurs. By extrapolation to a gas inlet temperature of 1500°K while retaining a constant cooling-air inlet temperature of 400°K, a value of blade relative temperature of 0·610 is predicted and corresponds to an average mean-diameter blade temperature of 1076°K (803°C).

The direct effect of gas-stream Reynolds number on the nozzle-blade cooling characteristic is demonstrated in Fig. 6, where average blade relative temperature at mean diameter is plotted against Reynolds number at various gas to coolant-air temperature ratios for a cooling-flow ratio of 0·02. From the curves it will be seen that a general reduction in cooling effectiveness occurs as the Reynolds number is reduced, in accordance with the detailed accounts in Refs. 2 and 3. The blade relative temperature at a Reynolds number of $0{\cdot}7 \times 10^5$ is 0·03 higher than the value at 2×10^5 for a gas to cooling-air temperature ratio of 3·0. Ref. 3 shows that when the cooling-flow ratio, gas temperature and cooling-air inlet temperature are maintained constant the conductance ratio, $h_g S_g / h_c S_c$, will vary in proportion to $(\mathrm{Re}_g)^{(n-0{\cdot}8)}$, where n is the exponent of the Reynolds number term in the expression for external heat transfer and can have values between 0·8 (turbulent flow) and 0·5 (laminar flow). Analysis of the variation of relative temperature versus Reynolds number in these turbine tests suggests that $n \simeq 0{\cdot}65$ for the nozzle blades at a temperature ratio of about 2·0 and therefore indicates that roughly equal areas of the blade external surface were covered by laminar and turbulent boundary layers respectively. The experimental curves for higher temperature ratios show a slightly less marked effect of Reynolds number on blade relative temperature, indicating a value of n greater than 0·65. This suggests that a greater proportion of the blade profile was covered by a turbulent boundary layer, i.e. transition probably occurred nearer the leading edge due to an increase of main-stream turbulence, itself caused by the rise in combustion temperature.

At a gas to cooling-air temperature ratio of 3·0, calculations showed that, for a gas-stream Reynolds number of 10^5, the coolant Reynolds number in the blade passage was approximately 2000*. Therefore, at lower Reynolds number, laminar flow in the coolant passages might have been expected with an attendant increase in the blade relative temperature[3]. This increase has not occurred, and suggests that the heat-transfer rates in the internal passages vary in a manner similar to that given by the formula for turbulent flow, viz. $Nu = 0{\cdot}02\ Re^{0{\cdot}8}$, even at Reynolds numbers lower than the commonly accepted transition value of 2300. A limited amount of experimental evidence[4], for flow in circular pipes with fully developed velocity and temperature profiles and with the surfaces appreciably hotter than the air bulk temperature, indicates that the transition Reynolds number (as defined by gas properties at bulk temperatures) may be as low as 1800.

The spanwise temperature distribution is illustrated in Fig. 7, where blade relative temperature is plotted against spanwise position for different cooling-flow ratios at a gas to cooling-air temperature ratio of 2·15 and at a Reynolds number of $1{\cdot}47 \times 10^5$. This particular test condition was selected because it was the only one in which the tip-section thermocouples operated satisfactorily. At the root and tip sections only three chordwise thermocouple positions were provided so that, to

---

* *See* Fig. 17.

obtain a comparable picture at the mean diameter, three thermocouples in similar chordwise positions were chosen. The increase in blade relative temperature from root to tip is as expected. The curve for zero cooling air was obtained, with the cooling passages blocked, at a Reynolds number of $1{\cdot}9 \times 10^5$ and shows the effects of conduction from the mid-span region to both blade root and tip. At this condition the experimental points indicate a mean external Nusselt number of 290 when compared with theoretical temperature distributions calculated by the method of Smith[7]. This is in good agreement with the value obtained from an equation based partly upon Ref. 5 but with the Reynolds number exponent derived from the present investigation. This equation is

$$Nu_g = 322 \left(\frac{Re_g}{2 \times 10^5} \right)^{0{\cdot}65}$$

The chordwise blade temperature variation is illustrated in Fig. 8 at various coolant-flow ratios for a Reynolds number of $1{\cdot}5 \times 10^5$ and a gas to cooling-air ratio of $3{\cdot}0$. As the coolant flow increases so the temperature variation across the blade chord increases. This may be due to the fact that the escape of cooling air from the leading edge of the blade into the clearance space at the inner diameter is progressively more restricted as the total coolant flow is increased. The cooling air then passes preferentially through the trailing-edge passages. The effect however is not serious up to a cooling-flow ratio of $0{\cdot}03$. The chordwise temperature distribution at a cooling-flow ratio of $0{\cdot}01$ showed good agreement with the results obtained by Hodge in Ref. 6.

4.2. *Nozzle-Blade Pressure-Drop Characteristic.*

Fig. 9a shows the measured pressure drop experienced by cooling air in flowing through the cooling passages under isothermal conditions, expressed in terms of the usual non-dimensional parameters. Points are plotted for a mean of a number of individual blades and for the whole nozzle ring assembly. In addition a curve is given of the calculated values assuming smooth pipe-flow friction coefficients. Good agreement is obtained between the individual blades and the theoretical calculation; the discrepancy between this and the nozzle assembly may be attributed to various small leakage paths between blades.

The nozzle-blade cooling-air pressure drop under turbine operating conditions may be expressed as

$$(\mathrm{P}_{CN} - \bar{p}_{SN})/(\mathrm{P}_i - \bar{p}_{SN})$$

where P_{CN} is the total pressure of cooling air in the nozzle header

$\bar{p}_{SN}$ is the mean gas static pressure at the nozzle blade tip (i.e. at the inner diameter)

P_i is the turbine gas inlet total pressure

When this non-dimensional parameter is greater than unity then $\mathrm{P}_{CN} > \mathrm{P}_i$ and further compression of the cooling air to pressures exceeding the compressor delivery pressure would be necessary in a gas-turbine engine. Under normal turbine operating conditions the cooling-air pressure drop in the nozzle blades for a given cooling-flow ratio and gas-flow Reynolds number will exceed the losses measured in a blade with no heat transfer. This extra pressure loss is caused by the heating of the cooling air which therefore has to be accelerated as it passes through the blade. If however the ratio of gas temperature to cooling-air temperature is increased, while the cooling-flow ratio and gas-flow Reynolds number are maintained constant, then the ratio of mean cooling-air density to

mean gas density will increase. This leads to a reduction in the ratio of mean cooling-air velocity to mean gas velocity and consequently to a reduction in the ratio of cooling-air pressure drop in the blade passages to gas pressure drop in the turbine stage.

This is shown on Fig. 9b where the pressure-drop ratio is plotted against cooling-flow ratio for different temperature ratios but comparable Reynolds numbers of approximately $1{\cdot}4 \times 10^5$. The change recorded is in fact small over the range of temperature ratio in which tests were made.

With the present system of construction in the turbine and at this Reynolds number, a cooling-flow ratio of approximately $0{\cdot}018$ may be achieved without the cooling-air inlet pressure exceeding the turbine inlet pressure. The corresponding average blade relative temperature at mid-span would be about $0{\cdot}6$ (Fig. 4). In other words a nozzle blade with this cooling configuration could be installed in a gas-turbine engine and run at an average mid-span temperature of 1120°K when the cooling-air and main gas inlet temperatures were 700°K and 1400°K respectively. At a Reynolds number of 5×10^4, the cooling-flow ratio would be expected to fall to $0{\cdot}015$; at 4×10^5 the corresponding cooling-flow ratio would rise to $0{\cdot}022$. For the same gas and cooling-air temperatures the average mid-span blade temperatures would be 1143°K and 1087°K respectively.

A further point arising from an examination of Fig. 9b is that the pressure-drop parameter, as plotted, does not fall to zero when no cooling air is passed through the blades. The explanation is that $\bar{p}_{SN}$ was an estimated value, assumed to be equal to the static pressure on the inner wall of the turbine annulus, just downstream of the nozzle blade row. This latter static pressure had to be obtained by calculation from the main-stream flow characteristics of the nozzle blades.

4.3. *Rotor-Blade Cooling Characteristics.*

As for the nozzle blade, the rotor blade relative temperature was defined as

$$\frac{\text{blade temperature} - \text{cooling-air inlet temperature}}{\text{'effective' gas temperature} - \text{cooling-air inlet temperature}}$$

In this case the 'effective' gas temperature was assumed to be equal to the calculated value of the total gas temperature relative to the rotor blades. Allowance was made for the reduction of main gas-stream temperature due to the addition of cooling air at points upstream of the rotor blade row. The rotor-blade cooling-air temperature was measured at the point where it entered the hollow shaft. As the rotor discs were well cooled by independent cooling-air supplies on the outer faces, the blade-cooling air picked up a negligible quantity of heat before reaching the blade roots. Furthermore the increment of total temperature given to the cooling air in being accelerated to the velocity of the cooling passages at the innermost diameter of the blade roots was approximately 4°C to 10°C for the speed range (6000 to 10 000 rev/min) in which the turbine was operated to obtain the rotor-blade cooling characteristics. Since this increment represents only a small correction to the cooling-air inlet temperature term (T_{cr}) in both the denominator and numerator of the expression for rotor-blade relative temperature, it was neglected in presenting the test results. The cooling-flow ratio was defined as the ratio of cooling-air mass flow passing through the cooling passages to the gas mass flow passing over the blades. Due to the ejection of cooling air into the main gas stream upstream of the rotor row, W_R was slightly greater than that passing through the nozzle row, W_N, at a given cooling-flow ratio.

The variation of average rotor-blade metal temperature (calculated in a similar fashion to the nozzle-blade average temperature) with cooling-flow ratio is shown on Fig. 10. As the observed effect of gas to cooling-air temperature ratio was small, plotted points are only given for ratios of

3·11, 3·41 and 4·63. At the highest value only a limited cooling-flow-ratio range was possible in view of the need to prevent the blade leading-edge temperature from exceeding 1270°K. An estimated curve is shown for a temperature ratio of 3·4, with an allowance for pumping work (Appendix IV) but assuming that there was no cooling of the blade by conduction along the span. The external heat-transfer rate assumed for this calculation was typical of those obtained in cascade tests[5] and is known (from Fig. 11) to be an under-estimate for the rotor blades under these turbine test conditions.

The reduction in cooling effectiveness at a constant cooling-flow and temperature ratio associated with a reduction in gas-flow Reynolds number is clearly shown in Fig. 11 for the present rotor blading, for a cooling-flow ratio of 0·02 and a gas to cooling-air temperature ratio of 3·41. In the range of Reynolds number covered in the tests ($6·5 \times 10^4$ to $1·53 \times 10^5$), the blade relative temperature changed from 0·66 to 0·62. Two theoretical lines are presented on this figure, calculated by the method of Ref. 3, using the Reynolds number exponent $n = 0·68$ and values of Nu_g^* equal to 430 and 330 respectively. The lower value of Nu_g^* is regarded as being typical of conditions with transition to a turbulent boundary layer only near the trailing edge on the convex surface. The higher value corresponds to transition on both surfaces, with a turbulent boundary layer over most of the concave surface. The experimental curve lies between these two theoretical curves, suggesting that a turbulent boundary layer was present on perhaps half the total blade surface and indicates an external Nusselt number of approximately 370 at $Re_g = 2 \times 10^5$. At given values of cooling-flow ratio and gas-flow Reynolds number, the cooling-air Reynolds number in the rotor-blade coolant passages exceeded the corresponding value obtained in the nozzle blades by approximately 40 per cent.† There was no clear evidence of transition to laminar flow in the coolant passages although the curves for the rotor blades appear to be somewhat steeper than those for the nozzle blades at gas-flow Reynolds numbers below 10^5.

The variation of blade relative temperature with gas to cooling-air temperature ratio is shown on Fig. 12 for a coolant-flow ratio of 0·02 and a gas-flow Reynolds number of 1×10^5. Experimental points are plotted for the mean surface and core temperatures along with estimates made by the method given in Appendix III. A general rise in relative temperature is noticeable as the gas to cooling-air temperature ratio increases, the values at 4·61 being approximately 8 per cent greater than those at 3·11.

Fig. 13 illustrates the variation of blade temperature along the span of the rotor blade at the leading and trailing edges for various cooling-flow ratios. There were insufficient thermocouples fitted to record the true average values. The increase in blade temperature from root to tip is immediately noticeable with the leading edge somewhat hotter than the trailing edge. The values at zero cooling flow agree fairly well with estimates by a method[7] which allows for conduction to the root of the blade.

The chordwise variation of relative blade temperature is demonstrated in Fig. 14 at a Reynolds number of 1×10^5 and a gas to cooling-air temperature ratio of 3·41, for various cooling-flow ratios. Now the gas-stream static pressure falls across the blade tip from leading edge to trailing edge. Therefore, as the cooling-flow quantity is reduced, the leading-edge passages tend to become starved of cooling air because the difference between the supply pressure and the exit pressure at the leading-edge tip tends to zero more rapidly than at other chordwise positions. The blade

† This is shown in Fig. 17.

leading-edge temperatures therefore approach the uncooled values at low coolant flows. As the feed pressure and therefore the coolant flow are increased, the distribution of cooling air improves and the temperature distribution becomes less skewed but by no means uniform. This sensitivity of the shape of the chordwise temperature distribution to cooling-flow ratio is in contrast with the behaviour of the shrouded nozzle blade.

Variation of the gas flow incidence on to the blade leading edge is shown to have only a slight influence on blade relative temperature in Fig. 15. Because of this it was possible in later tests to operate the turbine at a higher speed without setting up unrepresentative metal temperatures and thermal stress distributions.

4.4. *Rotor-Blade Pressure-Drop Characteristics.*

The pressure drop with isothermal flow through the rotor-blade cooling passages is shown on Fig. 16a in terms of the same non-dimensional parameters as those used for the nozzle blades. Again, for comparison, the calculated pressure drop for smooth pipe flow, assuming standard friction coefficients, is added. The curves show that end losses have only a small effect on the pressure drop.

Under turbine operating conditions the pressure drop through the rotor blades may be expressed non-dimensionally as

$$(P_{CR}-\bar{p}_{SR})/(P_i-\bar{p}_{SR})$$

where P_{CR} is the inlet total pressure of cooling air

$\bar{p}_{SR}$ is the mean static pressure at the rotor-blade tip

P_i is the turbine gas inlet total pressure.

When this non-dimensional parameter is greater than unity then $P_{CR} > P_i$ and further compression of the cooling air to pressures exceeding the compressor delivery pressure would be necessary in a gas-turbine engine. The measured relationship between this parameter and cooling-flow ratio is shown in Fig. 16b for various values of non-dimensional rotational speed and at various values of gas to cooling-air temperature ratio. At any given value of the pressure-drop parameter, an increase in cooling-air flow is obtained as the speed is raised. This would naturally be expected to reduce blade temperatures but at the same time it must be remembered that more work is done in pumping the cooling air which, for this reason, becomes hotter. Even so, a benefit of better cooling usually still remains. For example, from the pressure-drop characteristics given on Fig. 16b, the cooling flow that may be achieved without the cooling-air supply pressure having to exceed the turbine inlet pressure varies from $\phi = 0{\cdot}023$ at $N/\sqrt{T_{cr}} = 260$ to $\phi = 0{\cdot}031$ at $N/\sqrt{T_{cr}} = 580$. After making allowance for the pumping temperature rise using the method of Appendix IV the calculated average relative temperature at the mid-span of the blades falls from $0{\cdot}656$ to $0{\cdot}604$ as the speed increases. Without allowing for this pumping work done on the cooling air, the corresponding calculated values would be $0{\cdot}652$ and $0{\cdot}590$ respectively.

5. *Conclusions.*

The cooling performance of a set of extruded air-cooled turbine nozzle and rotor blades has been examined in an experimental turbine under the following test conditions:

Nozzle Blades

Gas-flow Reynolds number on to blades	$0{\cdot}7 \times 10^5$ to $3{\cdot}0 \times 10^5$
Inlet gas temperature	900°K to 1500°K
Blade cooling-flow ratio	0 to 0·03
Cooling-air inlet temperature	390°K to 420°K
Gas to cooling-air temperature ratio	2·0 to 3·5

Rotor Blades

Gas-flow Reynolds number on to blades	$0{\cdot}65 \times 10^5$ to $1{\cdot}6 \times 10^5$
Inlet gas temperature (to turbine stage)	900°K to 1500°K
Blade cooling-flow ratio	0 to 0·03
Cooling-air inlet temperature	290°K to 310°K
Gas to cooling-air temperature ratio	3·0 to 4·6

The following effects were noted.

(a) *Nozzle Blades.*

(i) The average relative temperatures of the nozzle blades have been measured over a range of gas-flow Reynolds numbers, from 7×10^4 to 3×10^5, for cooling-air flows up to 3 per cent of the main gas-stream flow at gas to cooling-air absolute temperature ratios from 2·0 to 3·0. At $Re_g = 2 \times 10^5$ and $T_g/T_{cr} = 3{\cdot}0$, an average blade relative temperature of 0·58 was measured at the mid-span for 2 per cent cooling-air flow.

(ii) Blade temperatures showed some sensitivity to gas-flow Reynolds number; with the cooling-flow ratio kept constant at 0·02, the blade relative temperature was increased by 0·03 by reducing the external Reynolds number on to the nozzle blades from 2×10^5 to 7×10^4.

(iii) The chordwise temperature distribution was non-uniform, particularly at higher cooling-flow ratios. It is believed that this non-uniformity was accentuated by the restriction imposed on the flow of cooling air through the leading-edge passages, as a result of providing a discharge path in the clearance space at the inner diameter. At high cooling flows, the cooling air tended to flow preferentially through the trailing-edge passages, which therefore were better cooled than those at the leading edge.

(iv) A change in the ratio of mean inlet gas temperature to cooling-air inlet temperature from 2·15 to 3·0 caused an increase of approximately 0·07 in the relative temperature of the blade. Only part of this may be attributable to temperature-ratio effects; it is possible that the boundary-layer transition points moved towards the leading edge due to increased main-stream turbulence at the higher gas temperatures. This would raise the rate of heat transfer from the gas stream to the blade surface.

(v) Reasonably good agreement with theoretical estimates at temperature ratios around 2·0 was obtained by assuming gas and blade heat-transfer rates comparable with those measured in a cascade tunnel. This indicates that approximately equal areas of the blade

surface were covered by laminar and turbulent boundary layers. From item (iv) it is possible that higher heat-transfer rates existed at higher temperature ratios, when the extent of the turbulent layer was increased.

(vi) The cooling pressure loss is such that in a gas turbine engine, a cooling-flow ratio of about 0·018 can be achieved with an inlet cooling-air pressure equal to the turbine inlet total gas pressure. This flow would confer an average relative temperature of approximately 0·6 at the mid-span, at a gas-flow Reynolds number of $1{\cdot}4 \times 10^5$.

(b) *Rotor Blades.*

(i) The cooling performance of the rotor blades has been measured over a range of gas-flow Reynolds numbers from $0{\cdot}65 \times 10^5$ to $1{\cdot}6 \times 10^5$, for cooling-air flows up to 3 per cent of the main gas-stream flow at gas to cooling-air absolute temperature ratios from 3·0 to 4·6. At $Re_g = 1 \times 10^5$ and $T_g/T_{cr} = 4{\cdot}63$, an average blade relative temperature of 0·66 was measured at the mid-span for 2 per cent cooling-air flow.

(ii) A Reynolds number effect was found similar to but rather more pronounced than that measured on the nozzle blades. With the cooling-flow ratio kept constant at 0·02, the blade relative temperature was increased by 0·03 by reducing the gas-flow Reynolds number on to the rotor blades from $1{\cdot}53 \times 10^5$ to $6{\cdot}4 \times 10^4$.

(iii) The chordwise temperature distribution was non-uniform, the leading edge exhibiting the highest metal temperature. This was caused partly by the lower available pressure drop through the blade at the leading edge, due to the fall in gas static pressure existing at the rotor-blade tip from leading edge to trailing edge. The remainder of the non-uniformity must be ascribed to the cooling-passage distribution within the blade section.

(iv) A small increase in blade temperature was recorded with increase in the ratio of mean gas temperature to inlet cooling-air temperature. Over the range from 3·11 to 4·63 an increase in blade relative temperature of 0·05 was measured.

(v) Fair agreement was obtained between practical results and theoretical estimates of relative temperature, provided somewhat lower values of Nusselt number were used than those quoted in earlier reports as giving typical heat-transfer rates from gases to blades in a turbine. This indicates that approximately equal areas of turbulent and laminar boundary layers existed over the blade surface.

(vi) Incidence of the gas flow on to the rotor blades had virtually no effect on the cooling performance.

(vii) The cooling-air pressure loss was such that a maximum cooling-flow ratio of approximately 0·031 could be obtained, with the present system of air supply, before the cooling-air inlet pressure became equal to the turbine inlet total-head pressure. This flow would give an average relative temperature of approximately 0·6 at the mid-span, for a gas-flow Reynolds number of 10^5.

REFERENCES

No.	*Author(s)*	*Title, etc.*
1	N. E. Waldren and J. A. Flint ..	Mechanical aspects of turbine blade cooling. Part I.—Description of an experimental high temperature turbine and associated test rig (cooled turbine No. 126). A.R.C. R. & M. 3404. December, 1962.
2	D. G. Ainley, N. E. Waldren and K. Hughes.	Investigations on an experimental air-cooled turbine—Parts I and II. A.R.C. R. & M. 2975. March, 1954.
3	D. G. Ainley	Internal air-cooling for turbine blades. A general design survey. A.R.C. R. & M. 3013. March, 1955.
4	J. F. Barnes	An experimental investigation of heat transfer from the inside surface of a hot smooth tube to air, helium and carbon dioxide. A.R.C. R. & M. 3246. March, 1960.
5	R. I. Hodge	A turbine nozzle cascade for cooling studies. Part II.—Comparison between measured and predicted mean Nusselt numbers at the blade surface. A.R.C. C.P. 493. May, 1958.
6	R. I. Hodge	The cooling performance of two extruded-type air-cooled turbine nozzle blades. A.R.C. C.P. 495. July, 1958.
7	A. G. Smith	Heat flow in the gas turbine. *Proc. Inst. Mech. Eng.*, Vol. 159. 1948.
8	C. G. Stanworth and D. S. C. Paine	Design and operation of the N.G.T.E. thermal shock analogue. A.R.C. C.P. 557. January, 1960.
9	W. A. Abbott	Unpublished M.o.A. Report.

APPENDIX I

Notation

A_b	Total cross-section area of blade profile
A_{core}	Cross-section area of blade core, defined in Appendix III
A_N	Area of cooling-hole passages in nozzle blade
A_R	Area of cooling-hole passages in rotor blade
B, C	Defined in Appendix III
K_p	Absolute specific heat of gas at constant pressure (ft. pdl/lb/°C in figures and in main text) (C.h.u./lb °C in Appendix II)
L	Total blade height
M_0	Gas Mach number at turbine nozzle outlet
Nu_g^*	Mean gas-flow Nusselt number when $Re_g = 2 \times 10^5$
P_{CN}	Total pressure of nozzle-blade cooling air at entry
P_{CR}	Total pressure of rotor-blade cooling air at entry
P_i	Turbine gas inlet total pressure
Re_g	Gas-flow Reynolds number (on to rotor or nozzle blades) based on blade chord, outlet velocity relative to the blade, and density and viscosity based on gas static temperature and pressure at blade outlet
S_c	Surface area of cooling holes in blade
S_g	Surface area of blade profile
T_{clc}	Turbine gas inlet total temperature (combustion-chamber delivery temperature)
T_{cr}	Cooling-air temperature at blade root
T_g	'Effective' gas temperature
T_m	Blade metal temperature
U_m	Rotor-blade speed at mean diameter
W	Main gas-stream flow
W_N	Main gas flow through nozzle blade row
W_R	Main gas flow through rotor blade row
X	Defined in Appendix III

b Sum of the minimum distances between adjacent cooling passages in the chordwise plane

h_c Heat-transfer coefficient from blade to cooling air (C.h.u./ft² °C sec)

h_g Heat-transfer coefficient from gas to blade surface (C.h.u./ft² °C sec)

l Distance measured along blade span from root

n Exponent of Reynolds number term in expression for external heat-transfer coefficient

$\bar{p}_{SN}$ Mean static pressure at nozzle-blade tip

$\bar{p}_{SR}$ Mean static pressure at rotor-blade tip

x Distance along blade profile measured from the leading edge

W_{CN} Coolant flow to nozzle blades

W_{CR} Coolant flow to rotor blades

ϕ_N Coolant flow to nozzle blades/main gas flow through nozzle blade row ($\phi_N = W_{CN}/W_N$)

ϕ_R Coolant flow to rotor blades/main gas flow through rotor blade row ($\phi_R = W_{CR}/W_R$)

APPENDIX II

Blade Details and Annulus Dimensions

	Nozzle	*Rotor*
Number of blades	29	40
Span l	3 in.	3 in.
Chord c	2·25 in.	1·62 in.
Maximum thickness	0·425 in.	0·40 in.
Leading-edge radius	0·10 in.	0·115 in.
Trailing-edge radius	0·04 in.	0·033 in.
Mean diameter	16 in.	16 in.
Mean diameter pitch s	1·73 in.	1·255 in.
Mean-diameter blade-passage throat	0·895 in.	0·749 in.
Stagger angle	36° 30′	22° 46′
Blade inlet angle	0°	15°
Blade outlet angle	58°	47° 30′
s/c mean diameter	0·77	0·775
Number of cooling passages	16	13
Total area of cooling passages per blade	0·0778 sq. in.	0·081 sq. in.
Total peripheral length of cooling passages per blade	6·24 in.	6·31 in.

APPENDIX III

The Calculation of Surface and Core Mean Blade Temperatures in an Air-Cooled Blade

It is assumed that the blade is cooled by passing cold air spanwise from root to tip in smooth internal passages of constant cross-section throughout their length.

For an element of the blade having a length δl at a distance l from the blade root, the basic differential equation for heat transfer is governed by the fact that the net rate of heat flow into the element is zero under steady state conditions. Therefore

$$\lambda_b A_b \frac{d^2 T_m}{dl^2} + h_g S_g (T_g - T_{ms}) + h_c S_c (T_c - T_{mc}) = 0 \tag{1}$$

where T_m is the average blade temperature across a chordwise section, T_{ms} is the average temperature of the external surface and T_{mc} is the average temperature of the cooling-passage surfaces.

The heat balance for the cooling passages may be written as:

$$w_c K_{pc} \frac{dT_c}{dl} + h_c S_c (T_c - T_{mc}) = 0. \tag{2}$$

The third equation governing the blade-cooling process is concerned with heat flow from the blade external surface to the cooling passages. This may be written in the form:

$$h_g S_g (T_g - T_{ms}) + \lambda_b F (T_{mc} - T_{ms}) = 0 \tag{3}$$

where $\lambda_b F$ represents the thermal conductance of the blade material between the external and internal surfaces.

The solution of these equations is simplified by assuming that conduction along the span of the blade is negligible. This condition is probably satisfied by air-cooled blades having aspect ratios of 2 or more, when constructed from heat-resistant materials. It is also assumed that T_g remains constant along the span of the blade.

Then if

$$\frac{h_c S_c}{h_g S_g} = X, \frac{w_c K_{pc}}{h_g S_g} = B.$$

$$\frac{\lambda_b F}{h_g S_g} = C, \frac{d^2 T_m}{dl^2} = 0,$$

$$T_{ms}' = T_g - T_{ms}, \; T_{mc}' = T_g - T_{mc},$$

and

$$T_c' = T_g - T_c,$$

equations (1), (2) and (3) become

$$T_{ms}' - X T_c' + X T_{mc}' = 0 \tag{4}$$

$$\frac{B}{L} \frac{dT_c'}{d\left(\frac{l}{L}\right)} - X T_{mc}' + X T_c' = 0 \tag{5}$$

$$T_{ms}' + C T_{ms}' - C T_{mc}' = 0. \tag{6}$$

The simplest solution to equations (4), (5) and (6) is obtained when variations in X, B and C along the blade span are ignored. X is the only term which is likely to vary appreciably because h_c will

increase from root to tip, particularly when a large degree of cooling is obtained from a small quantity of cooling air. In order to solve the equations in their simplified form with the least degree of error, mid-span values of X, B and C should be used.

From equations (4), (5) and (6) two differential equations may be derived from T_c' and T_{mc}' respectively.

$$\frac{dT_c'}{T_c'} = -\frac{L}{B}\left\{\frac{CX}{C+X+CX}\right\} d\left(\frac{l}{L}\right) \tag{7}$$

$$\frac{dT_{mc}'}{T_{mc}'} = -\frac{L}{B}\left\{\frac{CX}{C+X+CX}\right\} d\left(\frac{l}{L}\right) + \left\{\frac{C}{X(C+X+CX^2)}\right\} \frac{dX}{d\left(\frac{l}{L}\right)} d\left(\frac{l}{L}\right) \tag{8}$$

or since X is assumed to be invariant with l,

$$\frac{dT_{mc}'}{T_{mc}'} = -\frac{L}{B}\left\{\frac{CX}{C+X+CX}\right\} d\left(\frac{l}{L}\right). \tag{9}$$

The solutions to equations (7) and (9) are

$$\frac{T_c'}{T_{cr}'} = \frac{T_{mc}'}{T_{mcr}'} = e^{-k} \tag{10}$$

where

$$k = \int_0^{l/L} \frac{L}{B}\left\{\frac{CX}{C+X+CX}\right\} d\left(\frac{l}{L}\right)$$

$$= \frac{L}{B}\left\{\frac{CX}{C+X+CX}\right\}\frac{l}{L}. \tag{11}$$

Elimination of T_{ms}' from equations (4) and (6) gives an expression for T_{mc}' in terms of T_c', X and C which applies at all spanwise positions, including the root. Thus

$$T_{mcr}' = \left(\frac{(1+C)X}{CX+C+X}\right) T_{cr}' \tag{12}$$

so that

$$\frac{T_{mc}'}{T_{cr}'} = \frac{T_g - T_{mc}}{T_g - T_{cr}} = \frac{(1+C)X}{(CX+C+X)} e^{-k} \tag{13}$$

or

$$\frac{T_{mc} - T_{cr}}{T_g - T_{cr}} = 1 - \frac{(1+C)X}{(CX+C+X)} e^{-k}. \tag{14}$$

Similarly

$$\frac{T_{ms} - T_{cr}}{T_g - T_{cr}} = 1 - \frac{CX}{(CX+C+X)} e^{-k}. \tag{15}$$

Expressions for X and B have been derived in Ref. 3. In the term C the only remaining unknown quantity is F, the thermal conductance of the material between the blade external surface and the internal surfaces of the cooling passages. λ_b can usually be estimated with fair accuracy by making an assumption for T_m. The most reliable method for deducing F has been found at N.G.T.E. to be from measurements of simulated blade temperature on an analogue computer, described in Refs. 8 and 9. These measurements indicated that the average temperature of the core of the blade, defined as the area bounded by a line drawn through the centre of each cooling passage, was very

nearly equal to the average temperature of the cooling-passage surfaces. An expression for F was deduced from the study of the blades used on this turbine and other proposed designs. This was

$$F = \frac{2 \cdot 14\, S_g b}{(A_b - A_{\text{core}})} \tag{16}$$

and applies to cooled blades where the cooling passages are situated near to the external periphery of the blade chordwise section.

APPENDIX IV

A Method to Allow for the Temperature Rise Imported to Rotor-Blade Cooling Air Due to Pumping Action

Ref. 3 describes a method for obtaining calculated values of the average blade temperature at chosen spanwise positions in an internally air-cooled blade with cooling air flowing in one direction parallel to the spanwise axis. No allowance is made in this method for the fact that rotor-blade cooling air has pumping work done on it as it flows radially outwards and therefore undergoes a temperature rise due to this as well as to heat transfer from the main gas stream to the blade.

Applying a heat balance at any spanwise position and neglecting spanwise conduction of heat, one obtains

$$\frac{h_g S_g}{h_c S_c} = \frac{1}{X} = \frac{T_m - T_c}{T_g - T_m}. \tag{1}$$

Expressions for X are derived in Ref. 3.

It is assumed that in correcting for pumping temperature rise this ratio X remains unaltered although of course T_c and T_b are changed. By re-arrangement, it follows that

$$\frac{T_m - T_c}{T_g - T_c} = \frac{1}{X + 1} \tag{2}$$

also remains unaltered at any chosen spanwise position.

Now the pumping temperature increment to be added to T_c* is

$$\Delta T_c = \frac{U^2}{2Kp} \tag{3}$$

where U is the value of blade speed corresponding to the chosen spanwise position and the rotational speed.

Applying ΔT_c to the expression for blade relative temperature gives, after some re-arrangement, the result that

$$\left(\frac{T_m - T_{cr}}{T_g - T_{cr}}\right)' = \left(\frac{1}{X + 1}\right) + \left(\frac{\Delta T_c + T_c - T_{cr}}{T_g - T_{cr}}\right)\left(\frac{X}{X + 1}\right) \tag{4}$$

where the primed quantity is the blade relative temperature with an allowance for pumping temperature rise, and T_c is the calculated coolant temperature, without the allowance, obtained by the methods of Ref. 3.

---

* This assumes that the cooling air has no angular momentum immediately prior to entering the rotor assembly.

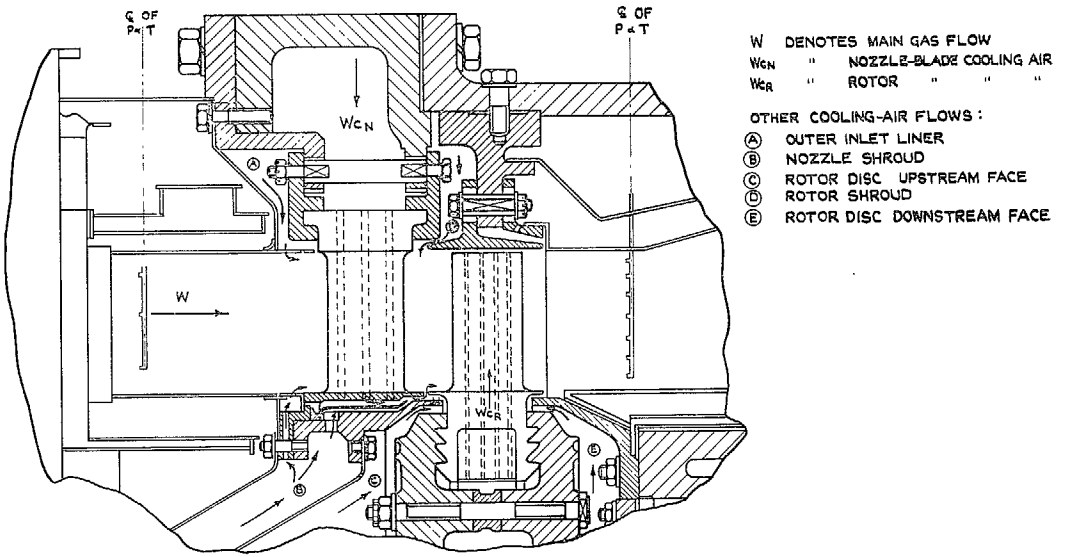

FIG. 1. Cooling-air flow through turbine stage.

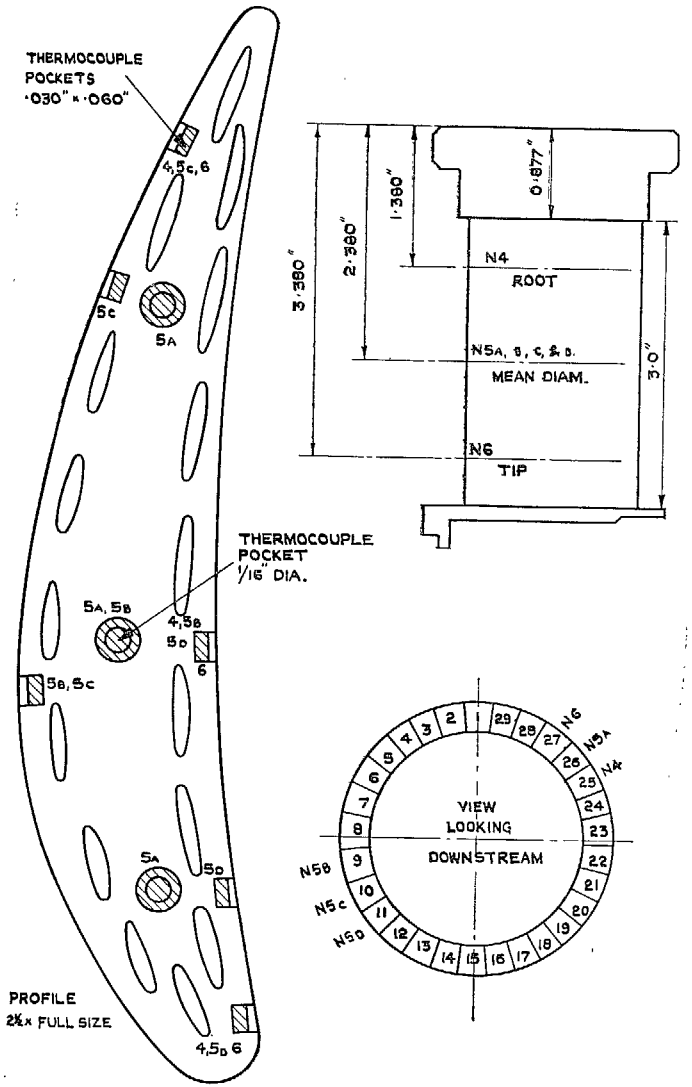

FIG. 2. Thermocouples in extruded nozzle blades.

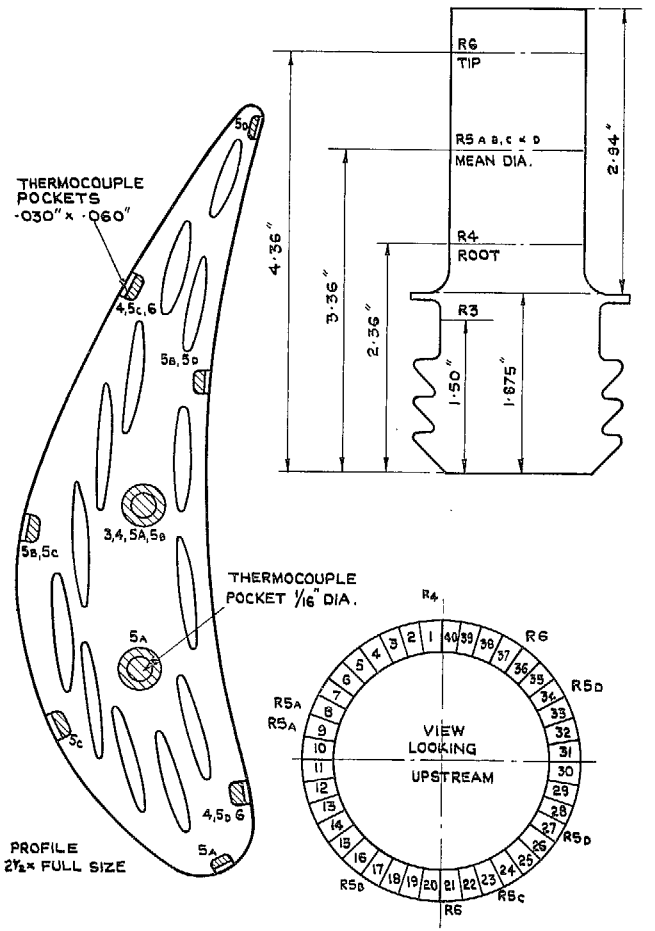

FIG. 3. Thermocouples in extruded rotor blades.

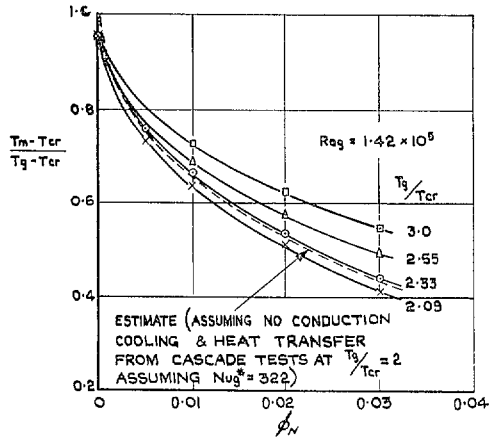

FIG. 4. Nozzle-blade average temperature at mean diameter *versus* cooling-flow ratio.

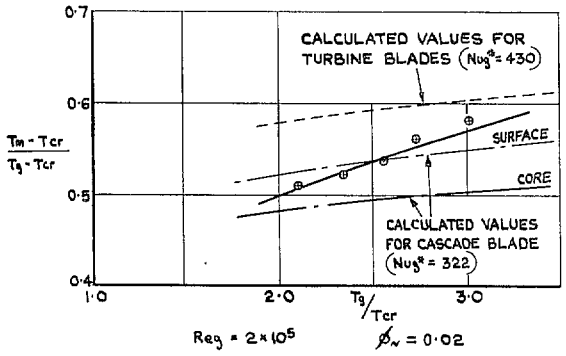

FIG. 5. Variation of average nozzle-blade temperature at mean diameter with temperature ratio.

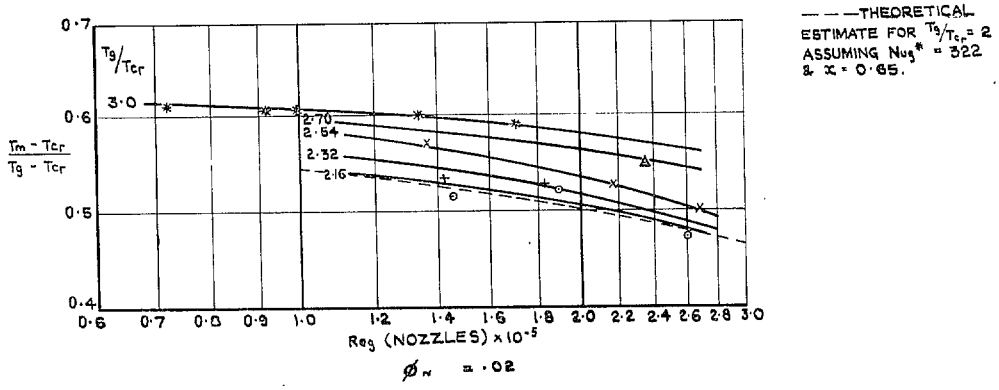

FIG. 6. Variation of average nozzle-blade temperature at mean diameter with Reynolds number.

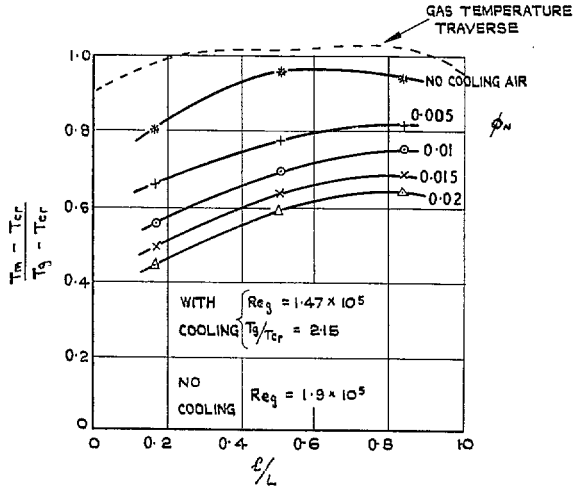

FIG. 7. Spanwise variation of nozzle-blade metal temperature.

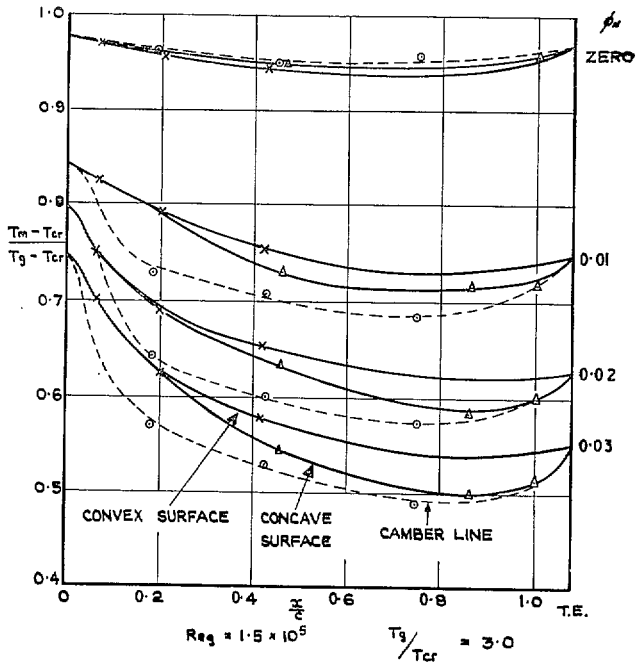

FIG. 8. Chordwise variation of nozzle-blade temperature at mean diameter.

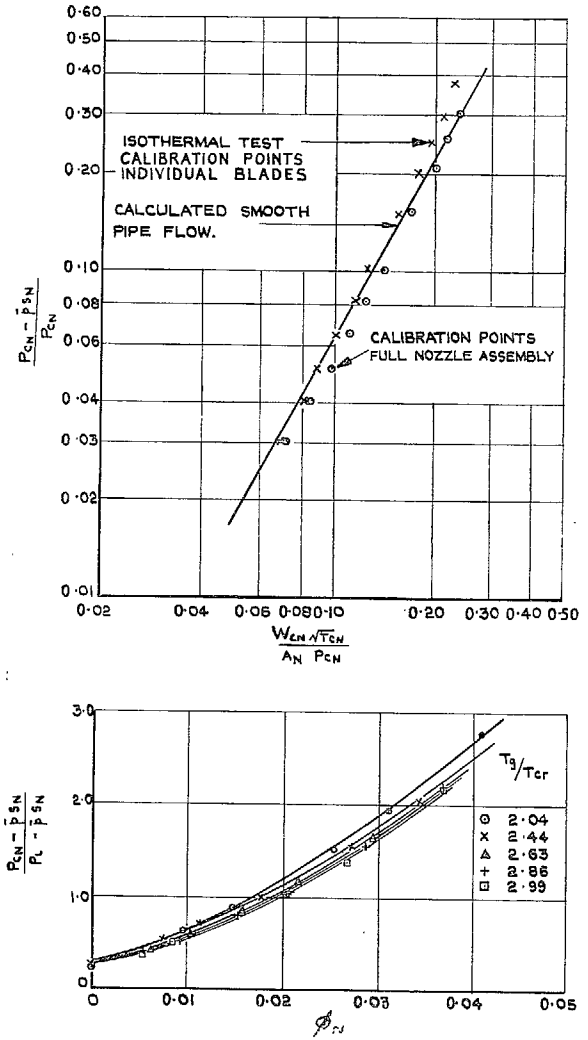

FIG. 9. Pressure drop through nozzle blade.

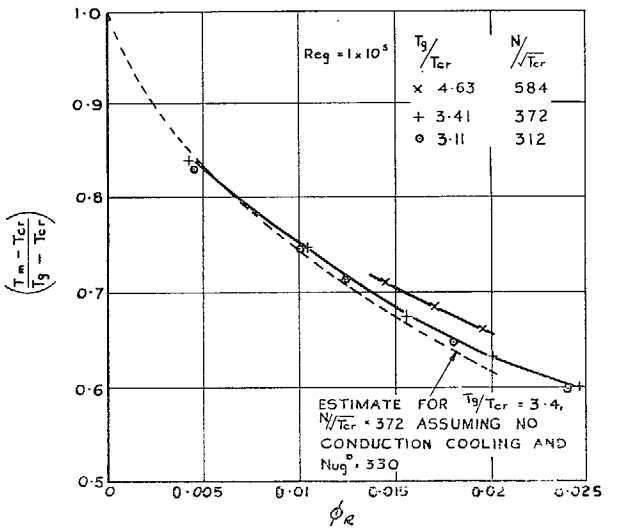

FIG. 10. Variation of average rotor-blade metal temperature at mean diameter with cooling-flow ratio.

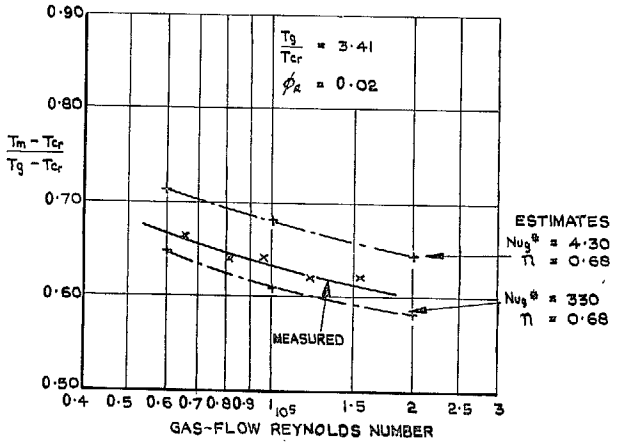

FIG. 11. Variation of average rotor-blade metal temperature at mean diameter with Reynolds number.

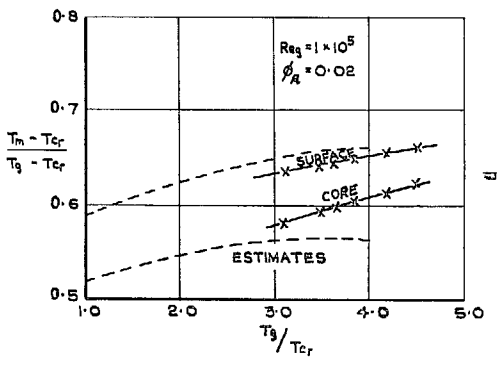

FIG. 12. Variation of average rotor-blade metal temperature at mean diameter with temperature ratio.

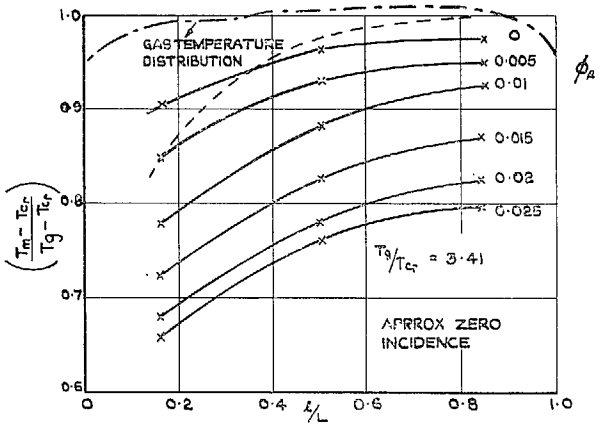

FIG. 13a. Variation of spanwise temperature distribution at leading edge with cooling flow.

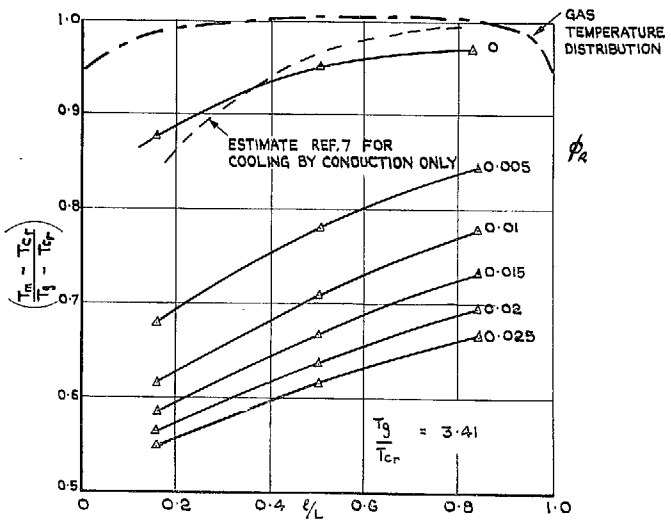

FIG. 13b. Variation of spanwise temperature distribution at trailing edge with cooling flow.

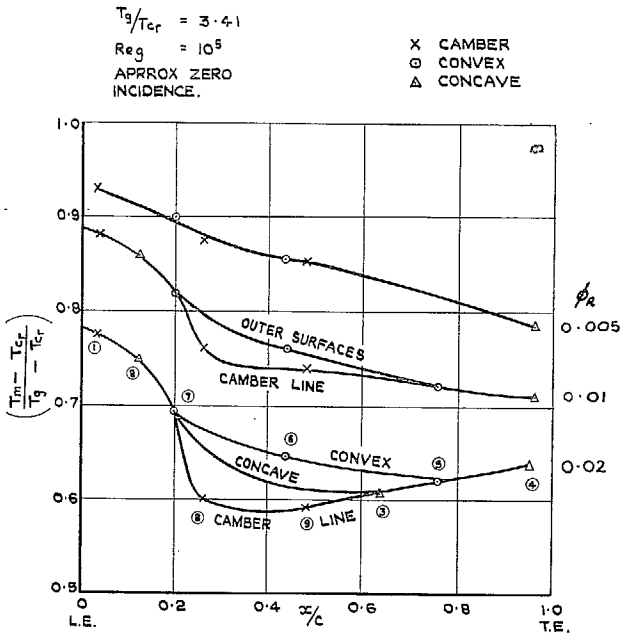

FIG. 14. Chordwise variation of rotor-blade metal temperature.

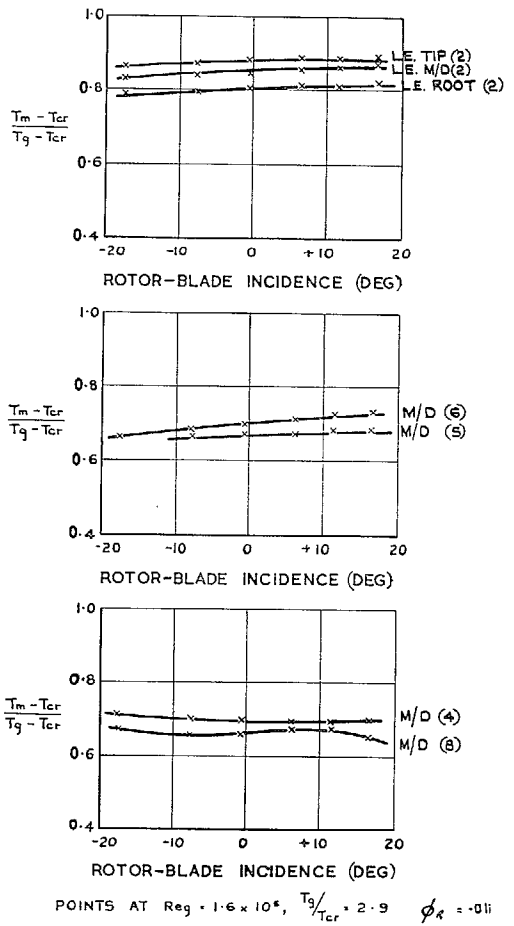

FIG. 15. Effect of incidence on rotor-blade metal temperature.

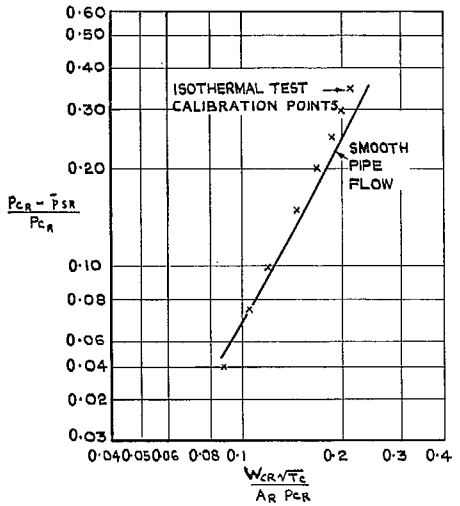

(a) RIG CALIBRATION OF A SINGLE BLADE.

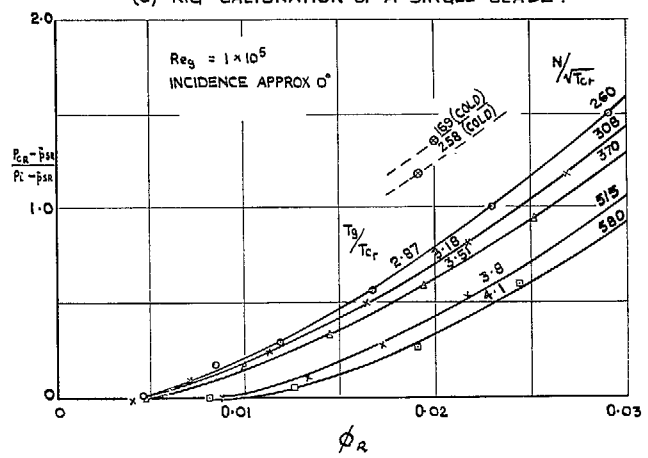

(b) AS MEASURED IN THE TURBINE.

FIG. 16. Pressure drop through rotor blade.

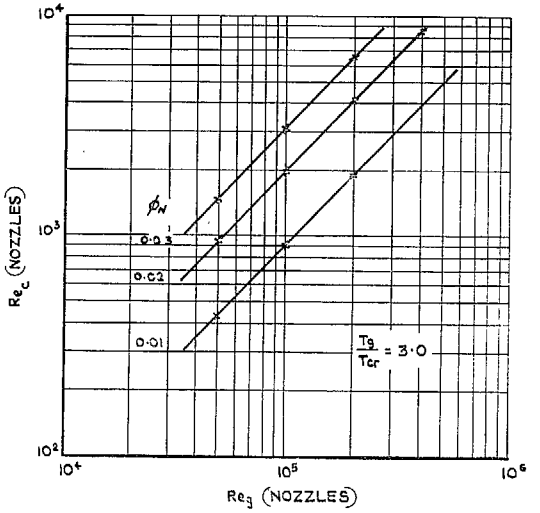

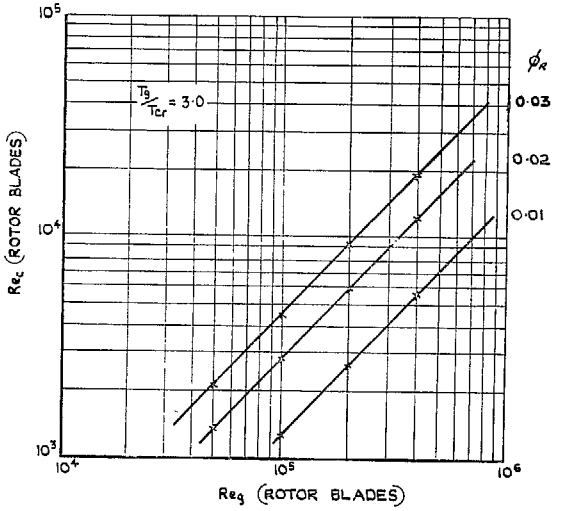

FIG. 17. Variation of coolant-flow Reynolds number with gas-flow Reynolds number.

Part II.—The Effects of Cooling on the Aerodynamic Performance

By J. F. Barnes and D. E. Fray

Summary.

Part II of this report describes tests conducted on the experimental high-temperature turbine at N.G.T.E. to measure the effects on aerodynamic performance of discharging cooling air into the main gas stream. The test results show the individual and combined effects on turbine isentropic efficiency of cooling-air discharge from each blade, from parts of the turbine annulus walls, from the rotor and nozzle shrouds and from the upstream face of the rotor disc.

Analysis of the test results has shown that the tip clearance losses associated with the unshrouded rotor blades in this turbine can be reduced to some extent when cooling air is discharged from the tips of the blades. Predictions based on a theoretical method, which allows for the changes in flow Mach number and angle and for the losses of total pressure and temperature due to mixing cooling air with the main gas stream, are in reasonable agreement with the observed efficiencies.

LIST OF CONTENTS

LIST OF APPENDICES

LIST OF ILLUSTRATIONS

1. *Introduction.*

Ref. 1 has given a description of the experimental high-temperature turbine (No. 126) and Part I of this report has presented the results of tests to determine the cooling characteristics of air-cooled nozzle and rotor blades manufactured by an extrusion process from billets of Nimonic 90 material. This report describes tests carried out on this turbine to measure the effects on aerodynamic performance of discharging cooling air into the main gas stream. Operation of a turbine at high gas inlet temperatures involves cooling parts of the turbine structure as well as the blades themselves. If the various cooling-air flows supplied to the blades and to parts of the turbine structure are discharged into the main gas stream, it must in general be expected that there may be attendant reductions in efficiency because the main gas stream is disturbed and pressure losses occur when the cooling air is mixed with the main gas stream. The test results presented in this report show therefore the individual and combined effects on turbine isentropic efficiency of cooling-air discharge from each blade row, from parts of the turbine annulus walls, from the rotor and nozzle shrouds and from the upstream face of the rotor disc.

An attempt has also been made to analyse the test data by employing a modified version of the standard method[2] currently used in turbine performance estimations at the National Gas Turbine Establishment. This analysis has shown that the tip clearance losses associated with the unshrouded rotor blades in this turbine can be reduced to some extent when cooling air is discharged from the tips of the blades.

2. *Description of Test Technique.*

The flow paths for the cooling air are shown on Fig. 1 of Part I. The cooling air from the sheet-metal liners forming the inlet annulus and part of the cooling air supplied to the nozzle shroud enter the main gas flow just upstream of the nozzle blades. The remainder of the nozzle-shroud cooling air enters the main gas flow downstream of the nozzle row. The cooling air from the nozzle blades themselves also follows this path. Other cooling flows which enter the main gas stream in the space between the blade rows are those from the upstream face of the rotor disc and from the rotor shroud. The rotor-blade cooling air is discharged into the clearance space existing between each blade tip and the rotor shroud. It then mixes with the main gas stream.

Cooling air from the rear face of the rotor disc and from holes in the walls of the exhaust annulus mixes with the main flow downstream of the turbine. Most of this cooling air mixes with the main flow downstream of the exhaust total pressure rakes and its effect on efficiency cannot therefore be determined. The exhaust-annulus cooling air was, however, only necessitated by the nature of the rig and was not representative of an engine turbine.

Tests were conducted under 'cold flow' conditions, at a main-stream inlet temperature of 400°K, so that all the running clearances in the turbine would be known accurately, in particular the rotor-blade tip clearance. It was known from previous experimental experience[3] that operation with combustion caused variations in clearances due to differential thermal expansion, and therefore could produce changes in turbine aerodynamic performance which might be sufficient to mask any changes caused by cooling-air discharge. The cooling air was also supplied to the turbine at 400°K; the only exception was the rotor-blade cooling air, supplied at 310°K to avoid damage to thermo-couple wiring situated inside the turbine shaft.

The first tests, with no cooling air, indicated that the isentropic efficiency of the turbine was very sensitive to Reynolds number effects, as is shown in Fig. 1. Attempts to measure efficiencies at lower

Reynolds numbers under cold-flow conditions with no cooling air did not meet with much success. Such Reynolds numbers could only be achieved with low air mass flows and output powers at inlet/outlet total pressure ratios close to unity: a wide scatter on measured efficiencies then became apparent. Subsequent tests for comparative purposes with and without cooling were all conducted at a main gas-stream Reynolds number on to the rotor blades of $3 \cdot 5 \times 10^5$. The following cooling flows given in Table 1 were applied independently.

TABLE 1

Cooling-Air Flows Expressed as Fractions of the Entry-Air Mass Flow

Nozzle shroud	0·008
Inlet liner	0·0033
Nozzle blades	0·0185
Rotor disc (upstream face)	0·0120
Rotor shroud	0·003
Rotor blades	0·0195

A test was also conducted with the following cooling-air quantities applied together. These were regarded as being representative of the cooling flows required under endurance-test conditions at an inlet gas temperature of 1500°K.

TABLE 2

Cooling-Air Flows Applied during Endurance Test, Expressed as Fractions of the Entry-Gas Mass Flow

Nozzle shroud	0·008
Inlet liner	0·004
Rotor disc (upstream face)	0·005
Nozzle blades	0·0245
Rotor shroud	0·004
Rotor blades	0·0195
Total	0·065

The gas-stream incidence on to the rotor blades was varied in each test by taking measurements at various speeds. The turbine isentropic efficiency was calculated from measurements of the main gas-stream and cooling-air flows, brake power, speed, inlet gas temperature and inlet and outlet total-head pressures. The definition of isentropic efficiency used in this investigation must be emphasised because different results for the effect of cooling-air discharge can be obtained according to the manner in which efficiency is defined.

As is well known, isentropic efficiency is generally defined as

$$\eta = \frac{[\text{Work temperature drop over stage}]}{\left[\begin{array}{c}\text{Isentropic temperature drop over stage for same} \\ \text{total pressures and inlet temperature}\end{array}\right]}.$$

Because the work temperature drop was obtained from measurements of brake horsepower and gas mass-flow rate, it was apparent that different values of work temperature drop could be obtained depending on whether or not cooling air was regarded as capable of producing power. In this experimental investigation and in the analysis that follows, all cooling air entering the main gas flow upstream of the rotor blade row was regarded as part of the working mass flow being expanded through the full main-stream pressure ratio and therefore contributed to the turbine power output. (*See* Appendix III.)

The experimental data for the effects of cooling-air discharge on isentropic efficiency are shown in Figs. 2 and 3 and are discussed further in Section 4.

3. *Description of Method of Analysis.*

In order to make comparisons between measured and calculated effects of cooling-air discharge over a wide range of turbine stage work parameter ($2K_p\Delta T/U_m^2$) it was first necessary to derive a relationship between rotor-blade loss coefficient and gas inlet angle so that the measured efficiencies with no cooling air agreed with those using the method of Ref. 2. The derived variation of loss coefficient (Y_{TR}) with gas inlet angle is shown as the upper curve in Fig. 4a. It applies when no cooling air is discharged from the rotor-blade tips.

The experimental and calculated effects of discharging nozzle-blade cooling air into the main gas stream are shown in Fig. 2. The method of calculation, given in detail in Appendix II, assumed, as in Ref. 2 that gas conditions at the mean diameter of the turbine annulus were always representative of the momentum mean conditions over the total annulus height. The main gas stream leaving the nozzle blade row was assumed to have suffered a loss of total pressure, in flowing past the blades, caused by profile loss, secondary losses, and trailing-edge effects. This pressure loss, together with the Mach number and gas outlet angle was calculated, using Ref. 2. The cooling-air discharge was regarded as a simplified process where mixing with the main stream occurred very quickly. Also it was assumed that the cooling air had no momentum parallel to the turbine axis and no angular momentum. As a result of these assumptions for mixing, the main gas stream suffered a change in Mach number, and reductions in total pressure and in the magnitude of the gas outlet angle. Expressions for these changes are given in Appendix II.

Comparison of the experimental points on Fig. 2 with the calculated curve for the discharge of 1·85 per cent nozzle-blade cooling air shows reasonable agreement. The same method can also be used to calculate the loss of efficiency occurring when cooling air is discharged into the main flow from the front face of the rotor disc. Comparison of Figs. 2 and 3 shows that the experimental effects for disc and nozzle-blade cooling air are similar, namely a loss of efficiency of approximately one point per cent for every one per cent of cooling air (relative to the main flow) discharged into the turbine annulus.

When cooling air was discharged from the rotor-blade tips, three different factors affecting the turbine power output had to be taken into account. These were (i) mixing losses, (ii) changes in the effective value of blade tip clearance and their effect on rotor-blade loss coefficient and gas outlet angle and (iii) the work done in pumping the cooling air through the passages in the blades in order to discharge it with a whirl velocity equal to the blade tip velocity. The first and third effects could be calculated, as is shown in Appendix II. The change in the effective value of tip clearance could only be deduced from test results by deriving a second blade loss-coefficient curve, as is shown in Fig. 4a, so that the calculated curve for the discharge of 1·95 per cent cooling air agreed as closely

as possible with the experimental points. The effective values of tip clearance corresponding to various points on this curve could then be found by a cross-plotting process. The expression for the effect of tip clearance on loss coefficient was assumed to be similar to that given in Ref. 2, but as a result of more recent test experience, the constant of proportionality was increased by a factor of 1·4 to make loss coefficients more sensitive to changes in tip clearance. These effective tip clearance values are shown on Fig. 4a.

Using this second derived curve of rotor-blade loss coefficient *versus* gas inlet angle, a final series of calculations was made to determine the effect of a total of 6·5 per cent cooling air distributed as indicated in Table 2. Once again Fig. 2 shows that the agreement between the experimental measurements and calculations was reasonable.

The method used to calculate the turbine power output, when cooling air is discharged from the rotor-blade tips, is given in Appendix III.

4. *Discussion.*

The effects of cooling-air discharge into the main gas stream cause reductions in the optimum value of isentropic efficiency, when this is defined on the assumption that cooling air entering the main flow upstream of the rotor blades is capable of contributing to the turbine power output.

These losses are given below:

TABLE 3

Measured Effects of Cooling-air Discharge on Isentropic Efficiency

Cooling-air quantity		Loss of efficiency at the optimum point
(a) Nozzle shroud	(0·008)	0·9 per cent
(b) Inlet liner	(0·0033)	0·4 per cent
(c) Nozzle blades	(0·0185)	1·8 per cent
(d) Rotor disc (upstream)	(0·0120)	1·1 per cent
(e) Rotor shroud	(0·003)	0·3 per cent (variable)
(f) Rotor blades	(0·0195)	0·6 per cent
(g) Combined effect	(0·065)	4·5 per cent

The apparent reduction in rotor-blade tip clearance when cooling air is discharged from the blade tips is evident not only from the deduced curve of loss coefficient given in Fig. 4a but from the small observed reduction in turbine efficiency. The pumping power expended on the cooling air would itself have caused a loss of efficiency approximately equal to 1·6 points per cent because it was nearly 2 per cent of the gross power output. In addition to this there must have been some losses caused by disruption of the main flow and by mixing. The discharge of 1·95 per cent cooling air, with only 0·6 points per cent measured loss in efficiency, has therefore caused a reduction in effective tip clearance which would have been sufficient to increase the efficiency by at least one point per cent. Similar effects were observed in Ref. 3 from tests on the 117 turbine where unshrouded nozzle blades were used as well as unshrouded rotor blades. Analysis of the 117 turbine

results indicated that, at zero incidence, the apparent reduction in tip clearance expressed as a fraction of blade height was approximately 0·005 for each blade row with 2 per cent cooling flow. The present analysis shows that this tip clearance/blade height ratio was reduced by 0·012, i.e. from 0·02 to 0·008, for a similar cooling flow.

An attempt was made to correlate these deduced reductions of tip clearance by calculating the penetration of the cooling-air jets into the clearance space using a rule[4] derived for the penetration of cooling-air jets into the main gas stream of a combustion chamber. The penetration, J, of such a jet is given by the empirical formula:

$$J = 1{\cdot}4 \left[\frac{\text{momentum of cooling jet}}{\text{momentum of main stream per unit area}} \right]^{1/2}.$$

For blades the momentum of the cooling jets could be estimated reasonably accurately but difficulties arose in calculating the momentum per unit area of the main stream. By making the very questionable assumption that this last quantity should be based on exit mean diameter conditions relative to the blade, some correlation was obtained between the experimental results for zero incidence and the calculated values of cooling-air penetration for each of the three blades. Attempts to allow for the effects of incidence met with little success and when it is remembered that the deduced changes of tip clearance have been obtained from small changes in values of measured efficiency, this is hardly surprising.

However, there is some support for the deduction from Fig. 4a that the tip-clearance sealing effect caused by cooling-air discharge is best when incidences are negative and relatively poor at positive incidences. This support arises from the fact that cooling air issuing from the blade tip would be swept away most easily in a direction perpendicular to the blade chord line. Under such conditions the tip-clearance sealing effect would be minimised and this condition is approached most closely at positive incidences.

Both the experimental and calculated results indicate that the effects of individual cooling air flows on turbine efficiency are not strictly additive. The loss of efficiency deduced from the individually measured effects would be 5·3 points per cent, whereas the actual measured loss is 4·5 points per cent.

This same non-additive characteristic is also true of the effects of cooling-air discharge on turbine inlet flow capacity. At a given pressure ratio and speed tests indicated that the turbine inlet flow capacity was reduced when cooling air was applied. Similar trends were obtained from calculations. Because the percentage reduction in flow capacity appeared to be independent of pressure ratio and speed, it is recorded in tabular form:

TABLE 4

The Effect of Cooling-Air Discharge on Turbine Inlet Flow Capacity

Cooling-air quantity		Per cent reduction in flow capacity	
		calculated	observed
Nozzle blades	(0·0185)	2·4	3·2
Rotor blades	(0·0195)	0	2·0
Combined flows	(0·065)	4·0	4·6

It would seem reasonable to assume that a given quantity of cooling air added with zero momentum to the main gas flow would cause the biggest change in swallowing capacity characteristics when it

was added at inlet to the turbine and that this change should progressively be reduced as the point of addition moved downstream. On this basis the discharge of cooling air upstream of the rotor blades would be expected to have a bigger effect than the discharge of the same quantity of cooling air downstream of the rotor. This is, in fact, observed. Moreover, the effect of varying the quantity of cooling flow added at a given point also appears to be non-linear. This is apparent when the observed reductions in flow capacity for 1·85 per cent nozzle cooling and 6·5 per cent cooling are compared. In the latter instance the cooling air entering the main stream between the blade rows is 3·75 per cent, so that if the effect were linear, a reduction in flow capacity of at least 6·4 per cent might be expected instead of the observed value (including the effects of other cooling-air discharges) of 4·6 per cent.

It has already been stated that the method used to calculate the effects of cooling-air discharge on turbine performance assumes an idealised mixing process which occurs very quickly and in which the cooling-air discharge has no momentum parallel to the turbine axis and no angular momentum. Because the method does not make any allowance for major flow disturbance and possible separation of the main-stream boundary layer at the point of injection, there is also the implicit assumption that the radial discharge velocity of the cooling air into the main stream is small. The limitations of this last assumption can be seen from an examination of Fig. 4b which shows the fractional loss of isentropic efficiency as measured on the N.G.T.E. single-stage model turbine (No. 113), for various axial clearances between the nozzle and rotor rows, when cooling air is discharged from the upstream face of the rotor disc. The analytical method described in this report agrees reasonably well with the observed results for the widest axial clearance on the 113 turbine and also for the discharge of nozzle-blade cooling air in the 126 turbine (Fig. 3). Presumably the increased radial velocity of discharge of the cooling air, caused by reducing the axial clearance between the nozzle and rotor rows at a given cooling flow, produces increased separation losses as shown on Fig. 4b. The analytical method, in its present form, cannot take account of this.

However, these results do tend to show that if cooling air can be discharged into the main stream with the smallest practicable radial velocity, the benefits to be gained in efficiency are appreciable. This argument can be taken further because it is clear that if cooling air could be discharged in the same direction and at the same total pressure and temperature as the main stream, no loss of efficiency would be recorded. These postulated conditions for cooling-air discharge could only be realised in a 'cold flow' test but the possibility of a reduction in losses by careful design of cooling-air discharge systems remains true in an engine.

A further point which emerges from the method for predicting mixing losses and which is relevant to engine operation is the fact that pressure losses, and changes of flow Mach number and angle are all proportional to the term $\{(W'\sqrt{T_t'})/(W\sqrt{T_t}) - 1\}$ where the primed symbols refer to conditions after mixing. When the cooling air is colder than the main stream, some reduction in the latter's total temperature must occur during mixing. Therefore under hot running conditions the changes in pressure, Mach number and angle might be expected to be slightly smaller than the corresponding changes applicable to a cold-flow test with the same cooling-flow ratios. The effects of these reductions in pressure loss on turbine efficiency are expected to be small and masked by the effects of changes in running clearances and Reynolds number.

Some indication of these last two effects can be seen in Fig. 5 where turbine efficiencies measured with 6·5 per cent cooling flow have been plotted against gas-flow Reynolds number on to the rotor blades. The plotted points have been taken from tests at various combustion temperatures for a range

of stage work-done parameter ($2K_p\Delta T/U_m^2$) between 2·0 and 3·3. Efficiencies are known to vary by no more than one point per cent, under cold-flow conditions in this range, as is shown on Fig. 2. The statistical variation of efficiency with Reynolds number, as deduced from the experimental points plotted on Fig. 5, has the equation:

$$1-\eta = 0{\cdot}216\left(\frac{1{\cdot}23\times10^5}{Re_g}\right)^{0{\cdot}145}$$

$$= \frac{1{\cdot}19}{Re_g^{0{\cdot}145}}$$

$$0{\cdot}6\times10^5 < Re_g < 1{\cdot}7\times10^5.$$

The curve representing this equation has been extrapolated to a Reynolds number of $3{\cdot}54\times10^5$ and is in good agreement with the results from the cold-flow tests. Each of the experimental points shown on Fig. 5 includes a correction for the effects of changes in the rotor-blade tip clearance. The corrections were calculated by a method given in Ref. 5, using measured shroud, blade and disc temperatures to assess the differential thermal expansion. The corrections applied varied between + 0·8 points per cent at a gas inlet temperature of 900°K ($Re_g \simeq 1{\cdot}6\times10^5$) to + 2·0 points per cent at 1500°K ($0{\cdot}6 < Re_g < 10^5$), with an average of + 1·3 points per cent.

As can be seen from the curves drawn on Fig. 5, effect of Reynolds number on efficiency with 6·5 per cent cooling air appears to be between the predictions of the formula due to Ackeret, viz.

$$\eta = 1-\tfrac{1}{2}(1-\eta_m)\left\{1+\left(\frac{3{\cdot}54\times10^5}{Re_g}\right)^{0{\cdot}2}\right\}$$

and that due to Moody:

$$1-\eta = (1-\eta_m)\left(\frac{3{\cdot}54\times10^5}{Re_g}\right)^{0{\cdot}2}$$

where η_m is the measured efficiency at a Reynolds number of $3{\cdot}54\times10^5$ and η is the required efficiency at any other Reynolds number. Curves representing these formulae have been shown on Fig. 5, for $\eta_m = 0{\cdot}815$, the peak value obtained under cold-flow conditions with 6·5 per cent cooling air.

Another factor which causes some loss of isentropic efficiency under engine running conditions has been discussed by Hawthorne[6]. It is the reduction in gas stagnation temperature caused by heat transfer to the surfaces of the blades. The loss of efficiency becomes progressively more marked as the blade temperature is reduced relative to the local gas temperature. For the experimental turbine stage under consideration where the ratio of blade absolute temperature to local gas absolute stagnation temperature has a minimum value of about 0·7, the maximum loss of isentropic efficiency will be about 1 percentage point and will occur at the lowest Reynolds number conditions shown on Fig. 5. At higher Reynolds numbers where the blade/gas temperature ratio will tend to unity, the loss will tend to zero.

Although this report is concerned primarily with the *changes* in turbine efficiency caused by cooling-air discharge, some comment on the absolute values of efficiency measured in these tests, and recorded in Fig. 5, is perhaps appropriate. It will be noted that under hot running conditions with 6·5 per cent cooling flow, isentropic efficiencies of 75 per cent were measured at Reynolds numbers around 10^5. The average pressure in the turbine stage under these conditions was only about 1·5 times the atmospheric value and therefore much less (perhaps by an order of magnitude)

than the pressures expected in an engine application. The Reynolds numbers in an engine would consequently be much higher and a gain of up to five points in efficiency might be expected from this alone. More careful choice of running clearances between the rotor-blade tips and the rotor shroud could easily produce a further bonus of one if not two points in efficiency, so that an efficiency of 81 or 82 per cent might be expected in an engine.

The influence of blade shape on efficiency must now be considered. The blades used in this turbine were untwisted and of constant section. This choice eased certain problems which existed when the blades were designed and which were associated with the extrusion of blade billets with fairly complicated cooling-passage configurations. The consequent compromise between aerodynamic requirements and manufacturing problems resulted in a rotor-blade form having a maximum thickness/chord ratio of 0·25 and a trailing-edge thickness/chord ratio of 0·04. Corresponding values for the nozzle blades are 0·019 and 0·036 respectively. A further concession in the aerodynamic design of the blades was to reduce their number in each row in order to minimise the total quantities of cooling air required. This resulted in pitch/chord ratios of approximately 0·77 in both blade rows.

Recent tests[7] in another single-stage turbine having very similar design velocity triangles have yielded information concerning the influence of trailing-edge thickness and blade pitching on turbine isentropic efficiency. These tests indicate that the sacrifice in efficiency due to the adoption in the cooled turbine of large trailing-edge thickness and pitching (compared with more usual thickness/chord ratios of about 0·01 to 0·015 and pitch/chord ratios of about 0·6 to 0·65) amounts to approximately three or four points per cent. It is probable also that the large values of maximum thickness/chord ratio, the large leading-edge radii, the generally poor aerodynamic forms of the blade profiles, the low blade aspect ratios and the absence of blade twist[8,9] may collectively cause a further loss of about two points in efficiency.

It would seem, therefore, that the present blade design involves a total sacrifice of five or six points in efficiency, which would be excessive if introduced in many engine applications. However it should be recognised that the prime objectives of the test series was to obtain basic information on heat-transfer characteristics and structural endurance of cooled turbine blades operating under conditions of extremely high gas temperature and low cooling-air temperature. For these objectives a high level of isentropic efficiency was only of secondary importance. With the aid of recent developments in manufacturing techniques and a slowly growing volume of information on blade-profile shapes for high efficiency, it should not now be necessary to sacrifice isentropic efficiency in a practical application of blade cooling to such a large degree. Nevertheless the present test data provide a clear indication that considerable caution must be exercised in finding an ideal compromise between blade form and internal cooling configuration (and hence the resultant temperature distribution) to meet a particular application.

In spite of the low efficiences measured on this turbine, the effects of cooling-air ejection particularly from the nozzle blades, can be regarded as realistic. As stated earlier they do show that mixing can occur between the cooling air and the main stream without causing serious disturbance of the latter's boundary layer. Furthermore, the theoretical model developed for the analysis of the test results shows that by careful design, the loss of total pressure fundamental to the mixing process can be minimised. If unshrouded rotor blades are used in an engine application, the effects of cooling-air discharge from the rotor blades, as measured in this investigation, are also of interest because they demonstrate a tip-clearance sealing effect.

5. *Conclusions.*

(1) When cooling air was discharged into the main gas stream, the isentropic stage efficiency of the high-temperature experimental turbine (No. 126) was reduced. If this efficiency is defined on the assumption that all cooling air entering the main gas flow upstream of the rotor blades is regarded as being capable of producing power (an assumption which demonstrates the efficiency reduction to the greatest possible extent), the following reductions in efficiency were measured at the optimum points:

Cooling-air quantity		*Loss of efficiency*
(a) Nozzle shroud	(0·008)	0·9 per cent
(b) Inlet liner	(0·0033)	0·4 per cent
(c) Nozzle blades	(0·0185)	1·8 per cent
(d) Rotor disc (upstream)	(0·0120)	1·1 per cent
(e) Rotor shroud	(0·003)	0·3 per cent
(f) Rotor blades	(0·0195)	0·6 per cent
(g) Combined effect	(0·065)	4·5 per cent

(2) The pumping power required to discharge the rotor-blade cooling air from the blade tips with a whirl velocity equal to the blade tip velocity was 2 per cent of the turbine power output and would have caused a loss of efficiency of 1·6 points per cent. The actual loss of efficiency was only 0·6 per cent and the difference is attributed to the reduction of the effective rotor-blade tip clearance when cooling air is discharged. The magnitude of this reduction has been estimated by a performance method which takes account of fundamental pressure losses due to mixing of the cooling air with the main gas flow. The actual degree of tip clearance reduction would seem to be sensitive to incidence, being small at positive incidences and greatest at negative incidences.

(3) The loss of efficiency measured when cooling air was discharged upstream of the rotor blades, e.g. from the nozzle blades, the front face of the rotor disc or from the rotor shroud, appeared to vary linearly with the actual quantity discharged. However, the corresponding reduction in inlet flow capacity, at a constant pressure ratio, was not proportional to the actual cooling flow. Similarly the individual measured effects of cooling-air discharge from various points in the turbine were not strictly additive: the combined effect was less than the sum of individual measurements.

(4) The method used to calculate the effects of cooling-air discharge on turbine performance assumes an idealised mixing process which occurs very quickly and in which the cooling air discharge has no momentum parallel to the turbine axis and no angular momentum. Because the method does not make any allowance for major flow disturbance and possible separation of the main-stream boundary layer at the point of injection, there is also the implicit assumption that the radial discharge velocity of the cooling air into the main stream is small. The agreement between the observed and calculated effects of discharging nozzle-blade cooling air indicates that very little, if any, additional separation occurred in this high-temperature turbine due to such discharge.

The same conclusion can be drawn by comparing the calculated and observed results for the discharge of cooling air from the upstream face of the rotor disc on the N.G.T.E. single-stage model turbine with a wide axial clearance between the blade rows. It would appear therefore that cooling air can be discharged into the main stream without separation occurring and without excessive pressure losses if some attention is paid to the design of discharge ports or slots so that the radial component of cooling-air discharge velocity is minimised.

(5) In the design of the experimental turbine no attempt was made to discharge the cooling flows deliberately with a substantial component of momentum in the direction of the local main-stream flow. An obvious rider to the present conclusions is that any such attempt (e.g. trailing-edge discharge of cooling air) would be of value in minimising mixing losses, where considerations of practical mechanical design permit this to be done.

REFERENCES

No.	*Author(s)*	*Title, etc.*
1	N. E. Waldren and J. Flint ..	Mechanical aspects of turbine blade cooling. Part I.—Description of an experimental high temperature turbine and associated test rig (cooled turbine No. 126). A.R.C. R. & M. 3404. December, 1962.
2	D. G. Ainley and G. C. R. Mathieson	A method of performance estimation for axial flow turbines. A.R.C. R. & M. 2974. December, 1951.
3	D. E. Fray and N. E. Waldren ..	Investigations on an experimental air-cooled turbine. Part III.—The effects of cooling on the overall turbine aerodynamic performance and initial operation at an inlet gas temperature of 1400 deg K. A.R.C. R. & M. 3144. January, 1958.
4	R. A. Jeffs and S. W. White ..	The performance of a combustion zone fed by a large number of small jets. N.G.T.E. Report R.209. A.R.C. 19 898. December, 1957.
5	D. G. Ainley and G. C. R. Mathieson	An examination of the flow and pressure losses in blade rows of axial flow turbines. A.R.C. R. & M. 2891. March, 1951.
6	W. R. Hawthorne	The thermodynamics of cooled turbines. Part I.—The turbine stage. *Trans. A.S.M.E.*, Vol. 78, No. 8, pp. 1765 to 1779. November, 1956.
7	I. H. Johnston and D. C. Dransfield	Unpublished work at N.G.T.E.
8	I. H. Johnston and L. R. Knight ..	Tests on a single-stage turbine comparing the performance of twisted and untwisted rotor blades. A.R.C. R. & M. 2927. February, 1953.
9	N. M. Markov	Research on turbine blade losses. Ref. M.O.A. Russian Abstracts No. 36. February, 1960.

APPENDIX I

Notation

A	Flow area, ft^2
H	Enthalpy, ft poundals/lb
J	Penetration, ft
K_p	Gas specific heat at constant pressure, ft poundals/lb°K
M	Mach number
P	Pressure, poundals/ft^2
R	Gas constant, ft poundals/lb°K
T	Temperature, °K
U	Blade speed, ft/sec
V	Gas velocity, ft/sec
W	Gas mass flow, lb/sec
Y_{TR}	Rotor-blade loss coefficient
h	Annulus or blade height, ft
k	Blade tip clearance, ft
n	Number of blades in a row
r	Radius, ft
s	Blade pitch, ft
α	Gas angle, radians
γ	Ratio of gas specific heat at constant pressure and constant volume
η	Isentropic efficiency
	Primed symbols (H, M, P, T, V, W, α, γ) denote conditions after mixing of cooling air.

Suffices

c	Cooling air (also, when used on cooling-air temperature and enthalpy, denotes conditions at inlet to the turbine system)
g	Gas
i	Conditions of the main gas flow at inlet to the turbine
m	Mean diameter conditions
s	Static conditions (pressure and gas temperature)
t	Total-head conditions (pressure and gas temperature)
w	Denotes whirl component of velocity
0	Gas conditions, relative to fixed coordinates, at exit from the nozzle blades
1	Entry gas conditions relative to the rotor blades
2	Exit gas conditions relative to the rotor blades
3	Gas conditions, relative to fixed coordinates, at exit from the stage

APPENDIX II

The Calculation of Changes in Gas-Flow Conditions when Cooling Air is Discharged into the Main Stream

General Considerations.

The solution of this problem involves the equations for the continuity of mass flow, conservation of momentum and conservation of energy. The equations for continuity of mass flow and the conservation of momentum depend on the details of the flow, whereas it is possible to write the equation for the conservation of energy in a form which is independent of the details of the flow process under investigation, provided it is assumed that energy is transferred from the main gas flow to the cooling air only during mixing and that no heat is lost from the system.* On this basis:

$$WH + W_cH_c = W'H' = (W+W_c)H' \tag{1}$$

or

$$WK_pT_t + W_cK_{pc}T_{tc} = W'K_p'T_t' \tag{1a}$$

where H_c and T_{tc} are the enthalpy and total temperature of the cooling air at entry to the turbine system. This assumption for the temperatures before mixing is convenient and is exact when the cooling air and main gas-stream temperatures are equal, as in a 'cold flow' test.

By using equation (1) or (1a), the total temperatures before and after mixing are known, together with the mass flows and the total pressure of the main stream before mixing, which is assumed to occur in an infinitesimally short distance so that changes of flow cross-section area can be neglected.

Detailed Considerations.

(a) *Cooling-air discharge upstream of a nozzle blade row.*

Before mixing occurs, the mass-flow equation can be written as

$$W_i = P_{si}AM_i\sqrt{\frac{\gamma}{RT_{si}}} \tag{2}$$

and after mixing,

$$W_i + W_{ci} = W_i' = P_{si}'AM_i'\sqrt{\frac{\gamma'}{R'T_{si}'}}. \tag{3}$$

If friction is neglected, the static-pressure forces are equal to the rate of change of momentum so that,

$$P_{si}A + \gamma P_{si}AM_i^2 = P_{si}'A + \gamma' P_{si}'AM_i'^2 \tag{4}$$

or

$$P_{si}(1+\gamma M_i^2) = P_{si}'(1+\gamma' M_i'^2) = \text{constant}. \tag{5}$$

Equations (2) and (3) can be combined as

$$\frac{W_i\sqrt{T_{si}}}{M_iP_{si}\sqrt{\frac{\gamma}{R}}} = A = \frac{W_i'\sqrt{T_{si}'}}{M_i'P_{si}'\sqrt{\frac{\gamma'}{R'}}} = \text{constant}. \tag{6}$$

---

* Rotor-blade cooling air is an exception which is considered in Section (c).

Introducing the definition of total temperature and combining equations (5) and (6),

$$\frac{W_i\sqrt{(T_{ti})}\,(1+\gamma M_i^2)}{\sqrt{\left(\frac{\gamma}{R}\right)}\,M_i\left(1+\frac{\gamma-1}{2}M_i^2\right)^{1/2}} = \text{constant}. \tag{7}$$

This can be differentiated with respect to M, giving

$$\frac{1}{W_i\sqrt{(T_{ti})}}\frac{d(W_i\sqrt{T_{ti}})}{dM_i} = \frac{(1-M_i^2)}{M_i(1+\gamma M_i^2)\left(1+\frac{\gamma-1}{2}M_i^2\right)}. \tag{8}$$

Equation (8) can be used to find the change in Mach number during mixing because $(1/W\sqrt{T_t})d(W\sqrt{T_t})$ can be written $(W'\sqrt{T_t'}/W\sqrt{T_t}-1)$ provided that the ratio of cooling flow to main-stream flow is small, which is usual.

Introducing the definition of total pressure, equation (5) becomes

$$\frac{P_{ti}(1+\gamma M_i^2)}{\left(1+\frac{\gamma-1}{2}M_i^2\right)^{\gamma/(\gamma-1)}} = \text{constant}. \tag{9}$$

This also can be differentiated with respect to M, giving

$$\frac{1}{P_{ti}}\frac{dP_{ti}}{dM_i} = \frac{-\gamma M_i(1-M_i^2)}{(1+\gamma M_i^2)\left(1+\frac{\gamma-1}{2}M_i^2\right)}. \tag{10}$$

Finally, combining equations (8) and (10) into the form most convenient for the performance methods of Ref. 2, where the change of Mach number is not required to be known,

$$\frac{W_i\sqrt{T_{ti}}}{P_{ti}}\frac{dP_{ti}}{d(W_i\sqrt{T_{ti}})} = -\gamma M_i^2. \tag{11}$$

Equation (11) can be used in the form

$$\frac{P_{ti}'-P_{ti}}{P_{ti}} = -\gamma M_i^2\left(\frac{W_i'\sqrt{T_{ti}'}}{W_i\sqrt{T_{ti}}}-1\right). \tag{12}$$

For 'cold flow' turbine performance estimates where only comparisons with the experimentally observed influence of cooling-air discharge on aerodynamic efficiency and swallowing capacity are required, T_{ti}, T_{tc} and T_{ti}' can be regarded as equal, so that

$$\frac{dP_{ti}}{P_{ti}} = \frac{P_{ti}'-P_{ti}}{P_{ti}} = -\gamma M_i^2\frac{W_{ci}}{W_i} = -\gamma M_i^2\frac{dW_i}{W_i}. \tag{13}$$

(b) *Cooling-air discharge immediately downstream of a nozzle blade row.*

In addition to changes in Mach number and total pressure, the change in gas outlet angle relative to the blade row is required. For this purpose, the equation for the conservation of angular momentum must be solved in conjunction with the others.

It is assumed that mixing occurs very quickly at the point of injection of the cooling air. Conditions at the mean diameter are assumed to be representative of the flow over the whole blade height. The cooling air is regarded as having zero momentum parallel to the turbine axis and zero angular momentum. The main-stream gas leaving the blade passage is assumed to have suffered a reduction

of total pressure, in flowing through the blade, caused by profile loss, secondary losses, tip-clearance effects (if any) and trailing-edge effects. On this basis the exit velocity V_0 and gas angle α_0 at the mean diameter can be regarded as uniform over the blade pitch. After mixing, the velocity and angle are similarly regarded as uniform.

The equation for continuity of mass flow can be written as

$$\frac{W_0\sqrt{T_{s0}}}{\cos\alpha_0 M_0 P_{s0}\sqrt{\frac{\gamma}{R}}} = nsh = \frac{W_0'\sqrt{T_{s0}'}}{\cos\alpha_0' M_0' P_{s0}'\sqrt{\frac{\gamma'}{R'}}} = \text{constant} \tag{14}$$

where suffix $_0$ refers to conditions at exit from the nozzle row, as in Ref. 3.

Equating the rate of change of momentum in the axial direction to the static-pressure forces gives

$$P_{s0}sh(1+\gamma M_0^2\cos^2\alpha_0) = P_{s0}'sh(1+\gamma' M_0'^2\cos^2\alpha_0'). \tag{15}$$

Applying the conservation of angular momentum to the gas flow before and after injection of the cooling air and subsequent mixing,

$$W_0 V_0 r_m \sin\alpha_0 = W_0' V_0' r_m \sin\alpha_0'. \tag{16}$$

Because mixing is assumed to occur over an infinitesimally small distance, there is no change in mean radius so that equation (16) becomes, using equation (14) and the definitions of Mach number and total pressure

$$\frac{\gamma P_{t0}\cos\alpha_0\sin\alpha_0 M_0^2}{\left(1+\frac{\gamma-1}{2}M_0^2\right)^{\gamma/\gamma-1}} = \text{constant}. \tag{17}$$

Equation (15) can also be written in terms of total pressure as

$$\frac{P_{t0}(1+\gamma M_0^2\cos^2\alpha_0)}{\left(1+\frac{\gamma-1}{2}M_0^2\right)^{\gamma(\gamma-1)}} = \text{constant}. \tag{18}$$

Equations (14), (17) and (18) can be used with the conservation of energy to obtain α_0', M_0' (and hence V_0') and P_{t0}'. This is a trial and error process, and for the small changes involved when mixing of only small quantities of cooling air is considered, it is much more convenient to obtain, by differentiation, a series of expressions which can be used in finite difference form, viz.,

$$W_0\sqrt{T_{t0}}\frac{d\alpha_0}{d(W_0\sqrt{T_{t0}})} = -\sin 2\alpha_0\left\{\frac{1+\frac{\gamma-1}{2}M_0^2}{1-M_0^2\cos^2\alpha_0}\right\} \tag{19}$$

$$W_0\sqrt{T_{t0}}\frac{dM_0}{d(W_0\sqrt{T_{t0}})} = \frac{M_0(\cos 2\alpha_0+\gamma M_0^2\cos^2\alpha_0)\left(1+\frac{\gamma-1}{2}M_0^2\right)}{(1-M_0^2\cos^2\alpha_0)} \tag{20}$$

and

$$\frac{W_0\sqrt{T_{t0}}}{P_{t0}}\frac{dP_{t0}}{d(W_0\sqrt{T_{t0}})} = -\gamma M_0^2. \tag{21}$$

Graphs of expressions (19) and (20) for $\gamma = 1{\cdot}4000$ were plotted to facilitate analysis of the cold-flow tests.

(c) *Cooling-air discharge from the tips of rotor blades.*

Pumping work has to be done on the cooling air to force it through the blade passages which it leaves with a whirl velocity U_{tip}, the blade-tip speed. The pumping work done per pound of cooling air is easily shown[3] to be $[U_{\text{tip}}]^2$ so that its total temperature at exit from the rotor blades, neglecting heat transfer from the gas *via* the blade to the cooling air, is given by

$$T_{tc\,\text{exit}} = T_{tc} + \frac{U_{\text{tip}}^2}{K_p}. \tag{22}$$

Similarly the angular momentum possessed by one pound of cooling air when it leaves the blades is $r_{\text{tip}}\ U_{\text{tip}}$ in the direction of rotation of the blades, thus tending to impart negative swirl to the main gas flow downstream of the rotor.

It is assumed that the cooling air and main gas stream mix at the latter's mean diameter conditions. This means that the equivalent mean diameter conditions for the cooling air have to be obtained in order to perform the calculation for total pressure loss, and the changes in Mach number and gas outlet angle, in a similar fashion to the method described in the preceding section for mixing downstream of nozzle blades.

Applying the conservation of angular momentum, the equivalent whirl velocity of the cooling air at mean diameter is given by

$$V_{wcm} = \frac{r_{\text{tip}}\ U_{\text{tip}}}{r_m}. \tag{23}$$

From the conservation of energy, the total temperature referred to absolute coordinates will remain constant with radius. The equivalent static temperature of the cooling air at mean diameter is therefore

$$T_{scm} = T_{tc} + \frac{U_{\text{tip}}^2}{K_p} - \frac{1}{2}\frac{U_{\text{tip}}^2}{K_p}\left(\frac{r_{\text{tip}}}{r_m}\right)^2, \tag{24}$$

i.e.

$$T_{scm} = T_{tc} + \frac{U_m^2}{K_p}\left[1 - \frac{1}{2}\left(\frac{r_{\text{tip}}}{r_m}\right)^2\right]\left[\frac{r_{\text{tip}}}{r_m}\right]^2.$$

The equivalent whirl velocity relative to the blade at mean diameter is $V_{wcm} - U_m$, i.e.

$$U_m\left[\left(\frac{r_{\text{tip}}}{r_m}\right)^2 - 1\right].$$

The total temperature of the cooling air relative to the blade at mean diameter thus becomes

$$T_{tcm(\text{rel})} = T_{scm} + \frac{U_m^2}{2K_p}\left[\left(\frac{r_{\text{tip}}}{r_m}\right)^2 - 1\right]^2 \tag{25}$$

because the static temperature remains the same in changing from absolute to relative conditions. The expression for the relative total temperature of the cooling air reduces to

$$T_{tcm(\text{rel})} = T_{tc} + \frac{U_m^2}{2K_p}. \tag{26}$$

If it is assumed, as in previous sections of this Appendix, that all the heat transferred from the gas to the blade is in turn given to the blade cooling air, the energy equation for mean diameter conditions becomes

$$W_1 H_1 + W_{c2} H_c + \frac{W_{c2} U_m^2}{2} = W_2' H_2' \tag{27}$$

where suffices $_1$ and $_2$ refer to gas conditions relative to the rotor blades at inlet and outlet respectively.

Also the term for the angular momentum of the cooling air relative to the blade must be included in the equation:

$$- W_2 V_2 r_m \sin \alpha_2 + W_{c2} r_m U_m \left[\left(\frac{r_{\text{tip}}}{r_m} \right)^2 - 1 \right] = - W_2' V_2' r_m \sin \alpha_2' \tag{28}$$

using the sign convention of Ref. 3 for velocity triangles. It is a straightforward matter to calculate H_2' and T_{t2}' from the modified equation for the conservation of energy (27). However, equation (28) together with the equation for the conservation of momentum in the axial direction and the equations defining mass flow cannot be solved by a simple process with the aid of graphs, unless a rotating system of coordinates is used such that the cooling air has zero relative angular momentum. The whirl velocity of such a coordinate system at the mean diameter is given by equation (23) and all the gas conditions relative to this system at exit from the blade have to be calculated, using the method given in Section 6.2 of Ref. 2. The changes in gas angle, flow Mach number and the loss of total pressure can then be computed by equations (19), (20) and (21) and a further transformation is needed to obtain the absolute outlet conditions from the rotor.

The results of performing calculations by this method have been compared with those obtained by an approximate method in which the angular momentum of the cooling air in equation (28) is neglected and equations (19), (20) and (21) have been used directly relative to the rotor blade, with suffix '$_2$' replacing suffix '$_0$'. The approximate method was found to give acceptable accuracy and was much quicker. The expressions used for calculating turbine power output, for each method of calculating pressure losses downstream of the rotor blade row, are given in Appendix III.

(d) *Cooling-air discharge downstream of a rotor blade row.*

This last case refers to the mixing of cooling air for the downstream face of the rotor disc and liner cooling air with the main stream, whose initial flow conditions for the purpose of calculation, are the absolute values denoted by suffix '$_3$' in Ref. 2. The finite difference equations (19), (20) and (21) deduced for mixing downstream of a nozzle blade row can be used, with suffix '$_3$' replacing suffix '$_0$'.

APPENDIX III

The Calculation of the Net Power Output and the Efficiency of an Air-Cooled Turbine

The power output can be expressed as the rate of change of angular momentum experienced by the gas and the cooling air in passing through the rotor blade row at the reference or mean diameters multiplied by the blade angular velocity.

Using angular momenta relative to absolute coordinates, the equation for power output becomes (for a stage where the reference diameters at inlet to and at outlet from the rotor are equal)

$$\text{Power} = - U_m(- W_0' V_0' \sin \alpha_0' + W_3 V_3 \sin \alpha_3) \tag{1}$$

The sign convention for velocities and angles is the same as that of Ref. 2 and primed symbols denote conditions after mixing of cooling air.

When cooling air is discharged from the blade tips, the term $W_3V_3 \sin \alpha_3$ in equation (1) should be evaluated taking account of the angular momentum of the blade cooling air. If, following the method suggested in Appendix II, this angular momentum has not been allowed for, the equation for power output becomes:

$$\text{Power} = -U_m(-W_0'V_0' \sin \alpha_0' + W_3V_3 \sin \alpha_3) - W_{c2}U_{\text{tip}}^2 \tag{2}$$

where $W_{c2}U_{\text{tip}}^2$ is the power used in pumping the cooling air through the blade cooling passages.

Using the relationships:

$$W_0' = W_1,\ W_2' = W_3,\ W_2' = W_1 + W_{c2} \tag{3}$$

and

$$\tan \alpha_1 = \frac{U_m}{V_0' \cos \alpha_0'} - \tan \alpha_0' \tag{4}$$

$$\tan \alpha_3 = \frac{U_m}{V_2' \cos \alpha_2'} - \tan \alpha_2'. \tag{5}$$

Equation (1) can be transformed to

$$\text{Power} = -U_m(W_1V_1 \sin \alpha_1 - W_2'V_2' \sin \alpha_2') - W_{c2}U_m^2 \tag{6}$$

$$= -U_mW_1(V_1 \sin \alpha_1 - V_2' \sin \alpha_2') + W_{c2}U_m(V_2' \sin \alpha_2' - U_m). \tag{6a}$$

This equation can be set up by considering the rates of change of the angular momenta of the gas and cooling air at the reference diameter relative to the rotor.

Using equation (28) of Appendix II, equation (6) can be written as

$$\text{Power} = -W_1U_m(V_1 \sin \alpha_1 - V_2 \sin \alpha_2) - W_{c2}U_{\text{tip}}^2 \tag{7}$$

which is exact whatever method is used to derive gas conditions after mixing downstream of the rotor.

Of all the possible expressions for power output, equation (7) is probably the most convenient to use. In this equation there is the implication that only cooling air mixed with the main gas flow upstream of the rotor blades can be regarded as being capable of contributing to the turbine power output. This is in accordance with the definition of efficiency used in this and other investigations of the influence of cooling-air discharge on the isentropic efficiency of a turbine stage, namely,

$$\text{efficiency} = \frac{\text{Net Power}}{W_0'\Delta H_{\text{isen}}}. \tag{8}$$

The isentropic heat drop, ΔH_{isen}, is calculated for the same ratio of inlet to outlet total pressure as that obtained in the test and for an inlet temperature which includes the effect (if any) of mixing cooling air upstream of the rotor row, i.e. T_{t0}'. In the present investigation where cold air is used throughout, T_{t0}' is assumed equal to T_{ti}.

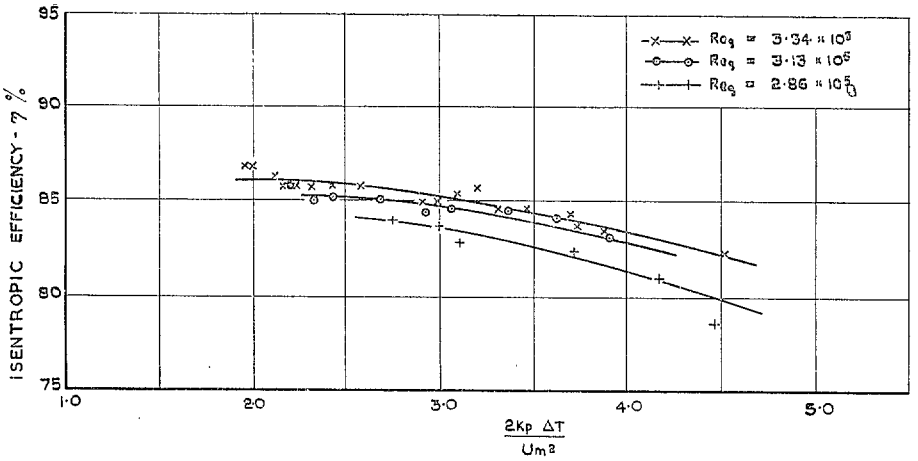

FIG. 1. Turbine isentropic efficiency—no cooling-air discharge.

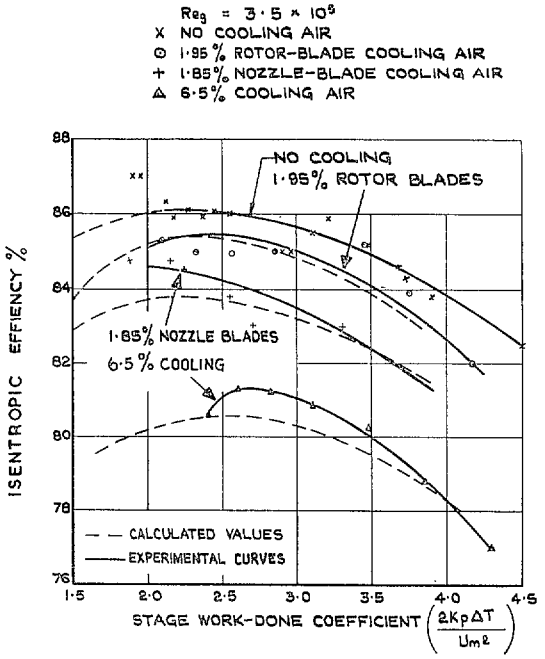

FIG. 2. Comparison between calculated and measured efficiencies.

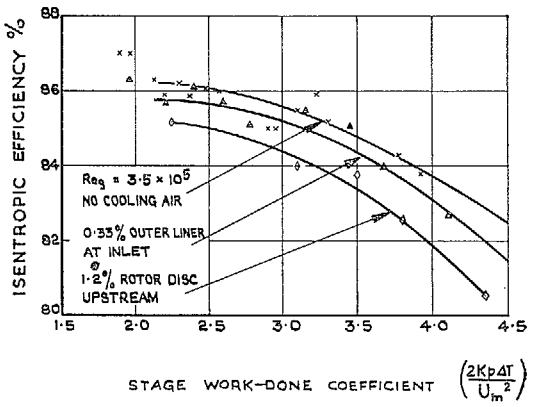

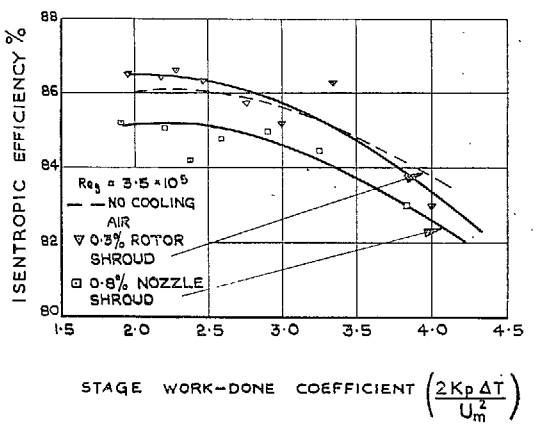

FIG. 3. Effect of cooling-air discharge on turbine isentropic efficiency.

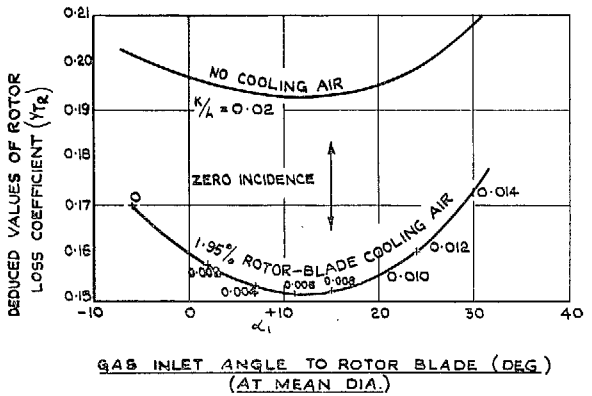

FIG. 4a. Deduced rotor-blade loss coefficients.

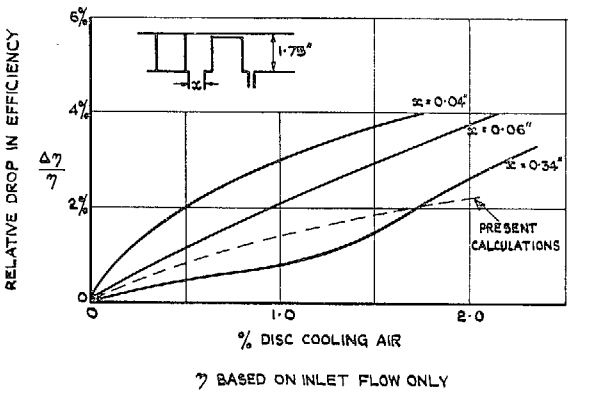

FIG. 4b. The effect of axial spacing on the loss of efficiency caused by discharge of disc cooling air.

(91497) Wt. 66/2301 K5 6/65 Hw.

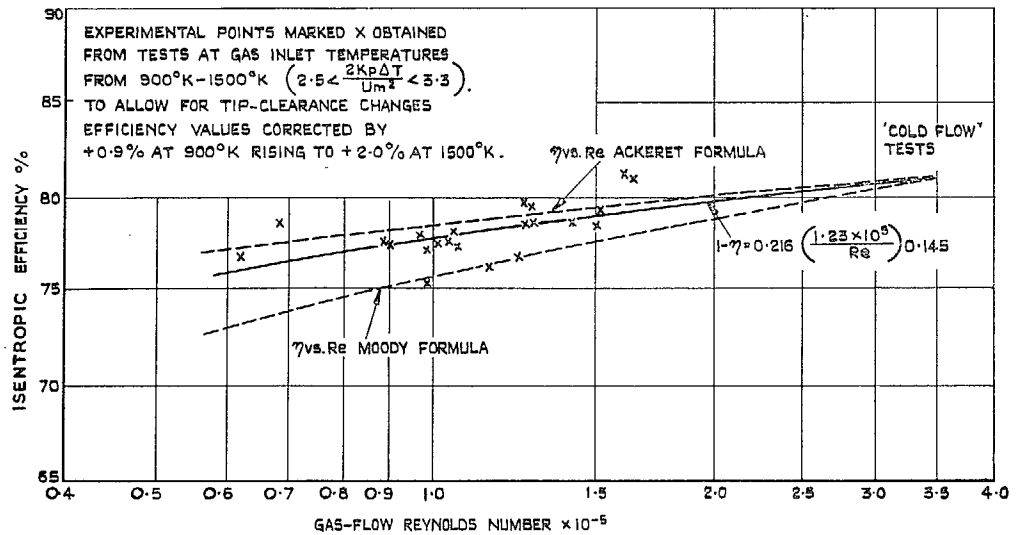

FIG. 5. Effect of Reynolds number on turbine isentropic efficiency with 6·5% cooling air.

Publications of the Aeronautical Research Council

ANNUAL TECHNICAL REPORTS OF THE AERONAUTICAL RESEARCH COUNCIL (BOUND VOLUMES)

1945 Vol. I. Aero and Hydrodynamics, Aerofoils. £6 10s. (£6 13s. 6d.)
Vol. II. Aircraft, Airscrews, Controls. £6 10s. (£6 13s. 6d.)
Vol. III. Flutter and Vibration, Instruments, Miscellaneous, Parachutes, Plates and Panels, Propulsion. £6 10s. (£6 13s. 6d.)
Vol. IV. Stability, Structures, Wind Tunnels, Wind Tunnel Technique. £6 10s. (£6 13s. 3d.)

1946 Vol. I. Accidents, Aerodynamics, Aerofoils and Hydrofoils. £8 8s. (£8 11s. 9d.)
Vol. II. Airscrews, Cabin Cooling, Chemical Hazards, Controls, Flames, Flutter, Helicopters, Instruments and Instrumentation, Interference, Jets, Miscellaneous, Parachutes. £8 8s. (£8 11s. 3d.)
Vol. III. Performance, Propulsion, Seaplanes, Stability, Structures, Wind Tunnels. £8 8s. (£8 11s. 6d.)

1947 Vol. I. Aerodynamics, Aerofoils, Aircraft. £8 8s. (£8 11s. 9d.)
Vol. II. Airscrews and Rotors, Controls, Flutter, Materials, Miscellaneous, Parachutes, Propulsion, Seaplanes, Stability, Structures, Take-off and Landing. £8 8s. (£8 11s. 9d.)

1948 Vol. I. Aerodynamics, Aerofoils, Aircraft, Airscrews, Controls, Flutter and Vibration, Helicopters, Instruments, Propulsion, Seaplane, Stability, Structures, Wind Tunnels. £6 10s. (£6 13s. 3d.)
Vol. II. Aerodynamics, Aerofoils, Aircraft, Airscrews, Controls, Flutter and Vibration, Helicopters, Instruments, Propulsion, Seaplane, Stability, Structures, Wind Tunnels. £5 10s. (£5 13s. 3d.)

1949 Vol. I. Aerodynamics, Aerofoils. £5 10s. (£5 13s. 3d.)
Vol. II. Aircraft, Controls, Flutter and Vibration, Helicopters, Instruments, Materials, Seaplanes, Structures, Wind Tunnels. £5 10s. (£5 13s.)

1950 Vol. I. Aerodynamics, Aerofoils, Aircraft. £5 12s. 6d. (£5 16s.)
Vol. II. Apparatus, Flutter and Vibration, Meteorology, Panels, Performance, Rotorcraft, Seaplanes. £4 (£4 3s.)
Vol. III. Stability and Control, Structures, Thermodynamics, Visual Aids, Wind Tunnels. £4 (£4 2s. 9d.)

1951 Vol. I. Aerodynamics, Aerofoils. £6 10s. (£6 13s. 3d.)
Vol. II. Compressors and Turbines, Flutter, Instruments, Mathematics, Ropes, Rotorcraft, Stability and Control, Structures, Wind Tunnels. £5 10s. (£5 13s. 3d.)

1952 Vol. I. Aerodynamics, Aerofoils. £8 8s. (£8 11s. 3d.)
Vol. II. Aircraft, Bodies, Compressors, Controls, Equipment, Flutter and Oscillation, Rotorcraft, Seaplanes, Structures. £5 10s. (£5 13s.)

1953 Vol. I. Aerodynamics, Aerofoils and Wings, Aircraft, Compressors and Turbines, Controls. £6 (£6 3s. 3d.)
Vol. II. Flutter and Oscillation, Gusts, Helicopters, Performance, Seaplanes, Stability, Structures, Thermodynamics, Turbulence. £5 5s. (£5 8s. 3d.)

1954 Aero and Hydrodynamics, Aerofoils, Arrester gear, Compressors and Turbines, Flutter, Materials, Performance, Rotorcraft, Stability and Control, Structures. £7 7s. (£7 10s. 6d.)

Special Volumes

Vol. I. Aero and Hydrodynamics, Aerofoils, Controls, Flutter, Kites, Parachutes, Performance, Propulsion, Stability. £6 6s. (£6 9s.)
Vol. II. Aero and Hydrodynamics, Aerofoils, Airscrews, Controls, Flutter, Materials, Miscellaneous, Parachutes, Propulsion, Stability, Structures. £7 7s. (£7 10s.)
Vol. III. Aero and Hydrodynamics, Aerofoils, Airscrews, Controls, Flutter, Kites, Miscellaneous, Parachutes, Propulsion, Seaplanes, Stability, Structures, Test Equipment. £9 9s. (£9 12s. 9d.)

Reviews of the Aeronautical Research Council

1949–54 5s. (5s. 5d.)

Index to all Reports and Memoranda published in the Annual Technical Reports

1909–1947 R. & M. 2600 (out of print)

Indexes to the Reports and Memoranda of the Aeronautical Research Council

Between Nos. 2451–2549: R. & M. No. 2550 2s. 6d. (2s. 9d.); Between Nos. 2651–2749: R. & M. No. 2750 2s. 6d. (2s. 9d.); Between Nos. 2751–2849: R. & M. No. 2850 2s. 6d. (2s. 9d.); Between Nos. 2851–2949: R. & M. No. 2950 3s. (3s. 3d.); Between Nos. 2951–3049: R. & M. No. 3050 3s. 6d. (3s. 9d.); Between Nos. 3051–3149: R. & M. No. 3150 3s. 6d. (3s. 9d.); Between Nos. 3151–3249: R. & M. No. 3250 3s. 6d. (3s. 9d.); Between Nos. 3251–3349: R. & M. No. 3350 3s. 6d. (3s. 10d.)

Prices in brackets include postage

Government publications can be purchased over the counter or by post from the Government Bookshops in London, Edinburgh, Cardiff, Belfast, Manchester, Birmingham and Bristol, or through any bookseller

Printed and published by
HER MAJESTY'S STATIONERY OFFICE

To be purchased from
York House, Kingsway, London W.C.2
423 Oxford Street, London W.1
13A Castle Street, Edinburgh 2
109 St. Mary Street, Cardiff
39 King Street, Manchester 2
50 Fairfax Street, Bristol 1
35 Smallbrook, Ringway, Birmingham 5
80 Chichester Street, Belfast 1
or through any bookseller

Printed in England

S.O. Code No. 23-3405